

NASA TECHNICAL
MEMORANDUM



NASA TM X-2476

NASA TM X-2476

PERFORMANCE OF A SMALL
ANNULAR TURBOJET COMBUSTOR
DESIGNED FOR LOW COST

by James S. Fear
Lewis Research Center
Cleveland, Ohio 44135

1. Report No. NASA TM X-2476	2. Government Accession No.	3. Recipient's Catalog No.	
4. Title and Subtitle PERFORMANCE OF A SMALL ANNULAR TURBOJET COMBUSTOR DESIGNED FOR LOW COST		5. Report Date February 1972	
		6. Performing Organization Code	
7. Author(s) James S. Fear		8. Performing Organization Report No. E-6320	
9. Performing Organization Name and Address Lewis Research Center National Aeronautics and Space Administration Cleveland, Ohio 44135		10. Work Unit No. 132-15	
		11. Contract or Grant No.	
12. Sponsoring Agency Name and Address National Aeronautics and Space Administration Washington, D.C. 20546		13. Type of Report and Period Covered Technical Memorandum	
		14. Sponsoring Agency Code	
15. Supplementary Notes			
16. Abstract <p>Performance investigations were conducted on a combustor utilizing several cost-reducing innovations and designed for use in a low-cost 4448-N (1000-lbf) thrust turbojet engine for commercial light aircraft. Low-cost features included simple, air-atomizing fuel injectors; combustor liners of perforated sheet; and the use of inexpensive type 304 stainless-steel material. Combustion efficiencies at the cruise and sea-level-takeoff design points were approximately 97 and 98 percent, respectively. The combustor isothermal pressure loss was 6.3 percent at the cruise-condition diffuser inlet Mach number of 0.34. The combustor exit temperature pattern factor was less than 0.24 at both the cruise and sea-level-takeoff design points. The combustor exit average radial temperature profiles at all conditions were in very good agreement with the design profile.</p>			
17. Key Words (Suggested by Author(s)) Low-cost combustor Air atomization		18. Distribution Statement Unclassified - unlimited	
19. Security Classif. (of this report) Unclassified	20. Security Classif. (of this page) Unclassified	21. No. of Pages 40	22. Price* \$3.00

PERFORMANCE OF A SMALL ANNULAR TURBOJET COMBUSTOR DESIGNED FOR LOW COST

by James S. Fear
Lewis Research Center

SUMMARY

Performance investigations were conducted on a combustor utilizing several cost-reducing innovations. The combustor was of a size which would be appropriate for a 4448-newton (1000-lbf) thrust turbojet engine which might be suitable for commercial light aircraft. A simple, air-atomizing device was used for fuel atomization. Film-cooled combustor liners were made of perforated sheet. Relatively inexpensive material, type 304 stainless steel, was used throughout. The inner combustor housing wall was eliminated. The combustor was designed for 406 K (271° F) and 19.8-N/cm² (29.7-psia) inlet air conditions and 867 K (1100° F) exit temperature, corresponding to Mach 0.65 cruise at an altitude of 7620 meters (25 000 ft). At sea level takeoff, the inlet conditions were 452 K (353° F) and 38.5 N/cm² (55.8 psia), and the exit design temperature was 964 K (2175° F).

Combustion efficiencies at the cruise and sea-level-takeoff design points described were approximately 97 and 98 percent, respectively. Combustor isothermal pressure loss was 6.3 percent at the cruise-condition diffuser inlet Mach number of 0.34. Combustor exit temperature pattern factors were 0.208 and 0.239 at the cruise and sea-level-takeoff design points, respectively. The combustor exit radial temperature profiles at all conditions were in very good agreement with the design profile. The fuel-air ratio required for ignition was below 0.020 at a combustor inlet total pressure of 6.0 N/cm² (8.7 psia) or higher, but increased at lower pressures. Combustor inlet temperature at the windmilling test points was not simulated. Air at ambient temperature was used. A second combustor was tested, identical with the first, but with simplex fuel nozzles in place of the air-atomizing devices. This combustor was tested for comparison purposes and also because the simplex nozzles would be attractive for possible missile applications with limited fuel-flow ranges. The performance results of the two combustors were nearly identical.

INTRODUCTION

The use of turbojet and turbofan engines for large aircraft is now nearly universal. These engines are also attractive for use in light aircraft because they offer such potential advantages as compactness, light weight, and greater simplicity as compared with reciprocating or turboprop engines. Light aircraft performance could be improved by the use of turbojet and turbofan engines, with increased cruise speed and rate of climb. The major obstacle in applying the turbojet or turbofan engine to light aircraft use is the high cost of these engines. As part of the gas-turbine technology program at the NASA Lewis Research Center, studies have been made to examine the possibility of reducing the total manufactured cost of small turbojet or turbofan engines to one-quarter or less of the cost of current engines of similar thrust level (ref. 1). Such a drastic reduction in cost necessitates some compromises when weighing engine performance against initial cost. It also necessitates improved low-cost fabrication techniques coupled with design of engine components aimed at significant cost reduction.

As a result of studies of aircraft flight requirements, engine cycle characteristics, and design cost-reduction potential, both a turbojet engine and a turbofan engine were selected to serve as a focus for the technology program (refs. 1, 2, and 3). A turbojet engine with a sea-level thrust of 4448 newtons (1000 lbf) was selected for this investigation. The engine has a single-stage turbine and a four-stage axial compressor with a 4:1 compression ratio. The design cruise point is a flight Mach number of 0.65 at an altitude of 7620 meters (25 000 ft).

This report describes the design of the combustor for the selected turbojet engine and presents the results of combustor performance tests.

SCOPE OF INVESTIGATION

A combustor was designed and developed to meet the performance requirements of the proposed low-cost turbojet engine and, at the same time, to utilize cost-reducing design innovations. Some of these innovations are

- (1) The use of a plain perforated sheet liner for film cooling instead of scoops, louvers, etc.
- (2) The elimination of an inner combustor housing wall, using the engine rotating shaft instead
- (3) The elimination of costly duplex or variable-area fuel nozzles, using instead high-velocity combustor inlet air for fuel atomization
- (4) The use of type 304 stainless-steel material for all combustor parts

This combustor is referred to as "the air-atomizing combustor" (fig. 1 and table I).

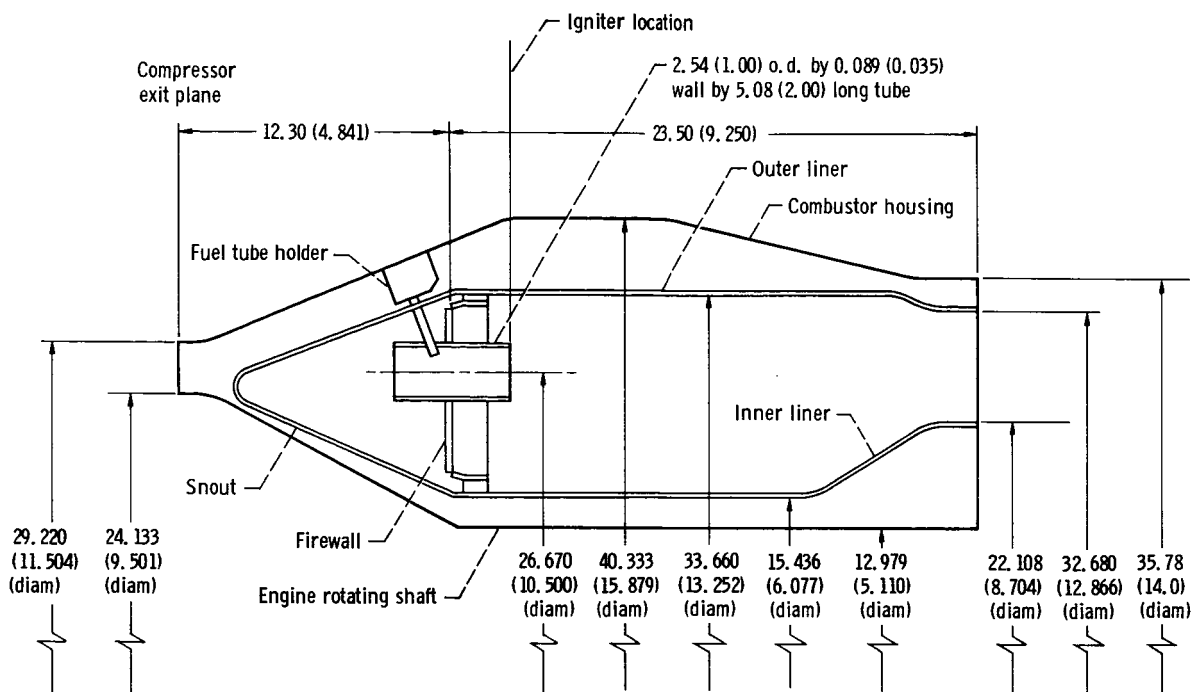


Figure 1. - Air-atomizing combustor. Dimensions are in centimeters (in.).

Performance data were obtained at three design points (table II) - sea-level takeoff, idle, and cruise at a flight Mach number of 0.65 and an altitude of 7620 meters (25 000 ft). Performance data were obtained also at a fourth point, a cruise point at the same Mach number and altitude as before but at combustor inlet conditions which would result from using a 6:1 compression ratio rather than a 4:1 ratio. This point is of interest because a low-cost turbofan engine might use a higher compression ratio.

A second combustor was fabricated, identical with the air-atomizing combustor, except that Monarch simplex fuel nozzles were used in place of the air-atomizing devices. This combustor is referred to as the "simplex nozzle combustor" and was built for the following two reasons:

(1) The simplex nozzle provides good fuel atomization over a narrower range of fuel flow, and the performance of this combustor in this fuel-flow range could be used as a benchmark for evaluation of the performance of the air-atomizing combustor.

(2) There is an interest in using low-cost turbojet engines in missile and drone applications having narrow ranges of fuel flow. The simplex nozzle is very attractive for these applications as it is inexpensive and can be sized for good fuel atomization at reasonably low fuel pressure.

For comparison purposes, performance data were obtained at the same three design points as with the air-atomizing combustor (table II). In addition, data were obtained at

a flight Mach number of 0.80 and an altitude of 6096 meters (20 000 ft), a flight condition of interest in a missile application.

All testing was conducted using ASTM A-1 fuel at ambient temperatures. Performance data included combustion efficiency; combustor total-pressure loss; combustor-exit temperature profiles; windmilling ignition data; and limited data on smoke formation, exhaust emissions, and durability.

The test facility and instrumentation used are described in appendixes A and B, respectively.

DESCRIPTION OF COMBUSTORS

Type of Combustor

The combustors tested were designed using the annular one-sided-air-entry approach described in references 4 and 5. In this approach, most of the combustion air enters through the outer combustor liner, with lesser amounts going through the combustor snout and firewall to aid in fuel atomization and to the inner combustor liner for cooling purposes only. Figure 2 shows a typical distribution of combustion air in a one-sided-air-entry combustor. There are no critical air splits between inner and outer annuli required to maintain recirculation and dilution zones in the combustor. Thus effects of radial distortions in compressor flow are minimized, and a suitable combustor exit temperature profile is achieved even at off-design conditions.

It has been found that small combustors do not operate as efficiently as larger combustors (ref. 6). This effect has been correlated as a function of the combustor hydraulic radius. The hydraulic radius of the one-sided-air-entry combustor can be maximized for a given combustor cross-sectional area by use of the space close to the rotating shaft. This is possible because only a narrow passage is required for the small amount of cooling air for the inner combustor liner. The hydraulic radius has been further increased, and weight and cost reduced, by the elimination of the inner combustor housing wall. The combustor inner liner cooling air flows between the liner and the rotating shaft, which functions as the inner housing wall.

Combustor Liner Design

The use of perforated sheet combustor liners was appealing from a cost viewpoint. The effectiveness of film cooling through the use of circular holes has been investigated

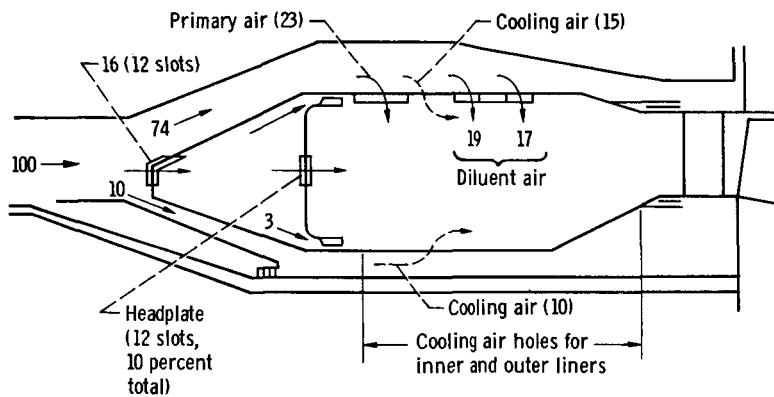
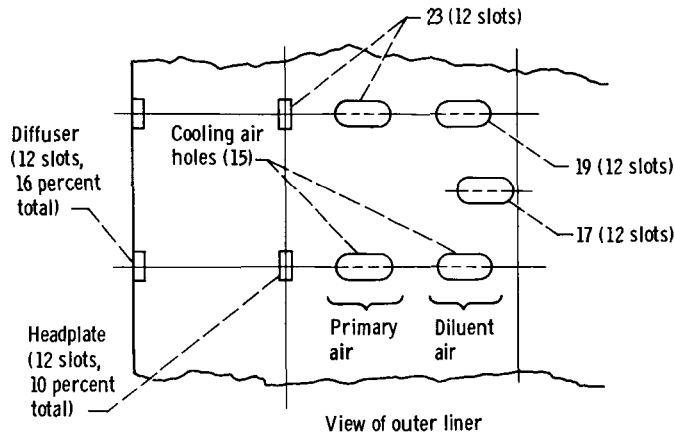


Figure 2. - Typical combustion air distribution in annular one-sided-air-entry type combustor. Numbers indicate percentages of total air flow rate.

and reported in reference 7. In using perforated sheet film cooling, two facts must be considered:

- (1) The cooling jet does not spread laterally to any appreciable extent.
- (2) If the jet has a high velocity, it will penetrate into the main air stream and not provide a high cooling effectiveness.

The lateral spread limitation can be overcome by proper orientation of the cooling hole pattern (fig. 3). It is necessary only that the hole pattern repeat by the time the jet is dissipated in the longitudinal direction. The cooling jets function most efficiently when the ratio of the momentum of the cooling stream to that of the main air stream is of the order of 0.5; however, fairly good efficiencies can be maintained with momentum ratios from approximately 0.2 to 0.8. This means that the perforated sheet method of film cooling will accommodate a wide range of diffuser efficiencies without severe deterioration of film cooling effectiveness.

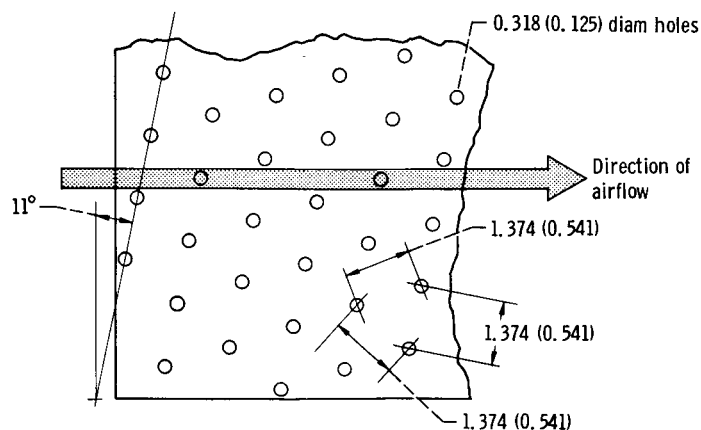


Figure 3. - Orientation of perforated sheet liner for optimum film cooling.
Dimensions are in centimeters (in.).

For good cooling effectiveness, it is generally advantageous to have many holes of smaller diameter, rather than fewer holes of larger diameter, for a given total open area. The particular hole pattern chosen was a compromise. The pattern shown in figure 3 is a relatively coarse one, and its selection was dictated by the consideration that fine hole patterns are difficult to manufacture in materials typically used in combustor liners. Preliminary tests showed this pattern to be satisfactory (ref. 8).

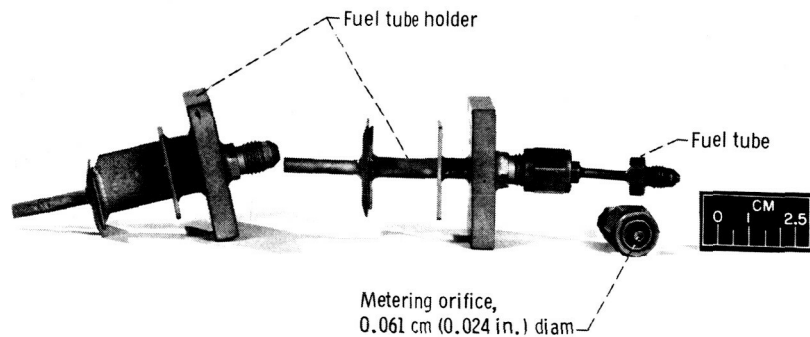
The primary-zone and dilution-zone air entry hole patterns were established on the basis of jet penetration theory and previous combustor design experience. The patterns used on the initial combustor liner design and the final design are shown in figure 4. Subsequent figures show the initial liner design, which differs from the final design only in the size of the primary-zone air entry holes. Two sets of secondary, or diluent, holes are used - one for deep penetration to the inner combustor liner, and the second for shallow penetration into the region near the outer liner. Plunged hole construction is used for added liner strength, as well as for improved hole discharge coefficients.

Ignition

Two surface-discharge-type igniters, 180° apart, were used. The ignition exciters were supplied with 24-volt dc electrical power and had an energy level of 20 joules.

Fuel Atomization

The only area in which the two test combustors differ is that of the method of fuel



C-71-1223

Figure 5. - Fuel tube holders and fuel tubes, showing metering orifice.

combustor, and not to atomize the fuel, it is probable that the fuel leaving the tubes is partially atomized. This is especially true at high fuel-flow rates, that is, with large pressure drops across the orifices. High-velocity air flowing through the cylinders completes the atomization and carries the fuel droplets into the primary combustion zone. The high-velocity air is obtained from the diffuser inlet passage by means of holes cut into the combustor snout opposite each fuel entry port. Performance parameters related to this method of fuel introduction, such as the effect of inlet air velocity on fuel droplet Sauter mean diameter, have not been studied; however, the inherently strong recirculation zone that is established in the one-sided-air-entry combustor should provide a long fuel residence time and make performance less sensitive to fuel droplet size.

Simplex nozzle combustor. - In the simplex nozzle combustor, fuel was introduced at 12 circumferential locations through Monarch simplex nozzles of the type customarily used in home oil furnaces. The nozzles were as shown in figure 6, with a flow rate of $0.0314 \text{ m}^3/\text{hr}$ (8.30 gal/hr) for each nozzle, at 69-N/cm^2 (100-psi) nozzle pressure drop. These nozzles were set in eight-bladed swirlers in the combustor firewall (fig. 7)



C-71-1222

Figure 6. - Monarch simplex fuel nozzle.

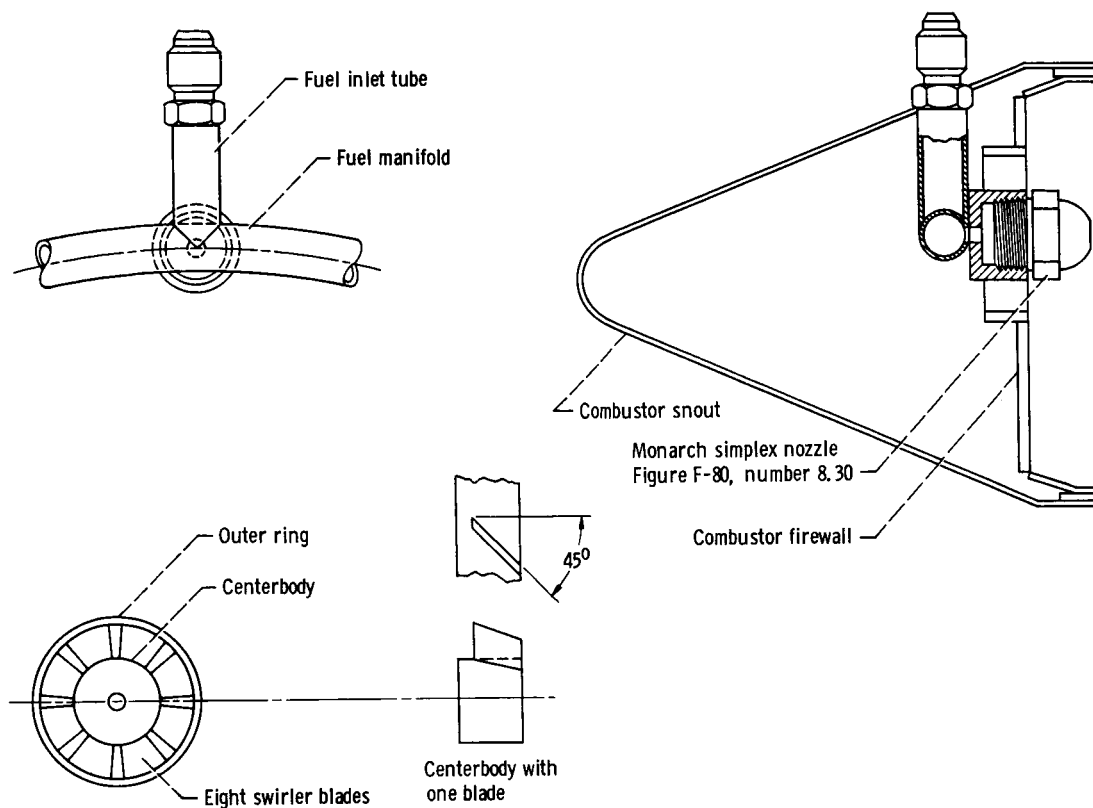


Figure 7. - Simplex nozzle combustor fuel manifold, nozzle, and swirler.

and were manifolded inside the combustor snout, with a single fuel tube supplying the fuel manifold.

CALCULATIONS

Combustion Efficiency

Combustion efficiency was calculated by dividing the measured temperature rise across the combustor by the theoretical temperature rise. The diffuser inlet temperature was taken as the arithmetic average of six thermocouple readings. The combustor exit temperature was taken as the arithmetic average of 65 thermocouple readings. Since the thermocouple rakes were not cooled and the surrounding combustor parts were at essentially the same temperature as the thermocouples, no radiation correction was required; and the indicated readings of the thermocouples were taken as true values.

Reference Velocity

Combustor reference velocity was calculated from the total airflow rate, the maximum cross-sectional area of the combustor housing, and the air density based on the total pressure and total temperature at the diffuser inlet.

Total-Pressure Loss

The combustor total-pressure loss includes diffuser total-pressure losses and is defined as

$$\frac{\Delta P}{P} = \frac{(\text{Average diffuser inlet total pressure}) - (\text{Average combustor exit total pressure})}{\text{Average diffuser inlet total pressure}}$$

The total-pressure loss was calculated from the arithmetic averages of 10 total pressures measured at the diffuser inlet and of 10 total pressures measured at the combustor exit. The number of readings was limited by the number of pressure transducers available for data recording. Manometer tubes, giving 30 pressure readings at the diffuser inlet and 30 at the combustor exit, were used periodically as a check. The diffuser inlet Mach numbers used to correlate total-pressure loss were calculated from the diffuser inlet measured static pressure, total temperature, and cross-sectional area and from the total combustor airflow.

Exit Temperature Profile Parameters

Three parameters often used in evaluating the quality of combustor exit temperature profiles are considered. The first is the exit temperature pattern factor $\bar{\delta}$, defined as

$$\bar{\delta} = \frac{T_{\text{exit, max}} - T_{\text{exit, av}}}{T_{\text{exit, av}} - T_{\text{inlet, av}}}$$

where $T_{\text{exit, max}} - T_{\text{exit, av}}$ is the maximum temperature occurring anywhere in the combustor exit plane minus the average combustor exit temperature. The term $T_{\text{exit, av}} - T_{\text{inlet, av}}$ is used in all three parameters and is the average temperature rise across the combustor. This parameter considers the maximum positive difference between an individual temperature and the average temperature, but does not take into account the design radial temperature profile of the combustor. A temperature which

is higher than the average combustor exit temperature may be only slightly above the desired temperature at the midspan of a turbine blade, while the same temperature would be excessively high at the blade hub. Two parameters which take the design profile into account are

$$\delta_{\text{stator}} = \frac{(T_{r, \text{exit, local}} - T_{r, \text{exit, design}})_{\text{max}}}{T_{\text{exit, av}} - T_{\text{inlet, av}}}$$

and

$$\delta_{\text{rotor}} = \frac{(T_{r, \text{exit, av}} - T_{r, \text{exit, design}})_{\text{max}}}{T_{\text{exit, av}} - T_{\text{inlet, av}}}$$

where $(T_{r, \text{exit, local}} - T_{r, \text{exit, design}})_{\text{max}}$ for δ_{stator} is the largest positive temperature difference between the highest local temperature at any given radius and the design temperature for that radius; and where $(T_{r, \text{exit, av}} - T_{r, \text{exit, design}})_{\text{max}}$ for δ_{rotor} is the largest positive or negative temperature difference between the average radial temperature at any given radius and the design temperature for that radius. In the case of δ_{stator} the maximum excess in local temperature is considered because a stator blade continuously "sees" this temperature; a rotor blade periodically passes through the region of high temperature, so that a point on a given radius of the rotor blade "sees" the average temperature for that radius. Thus the maximum difference in average temperature is used in calculating δ_{rotor} . Only a positive difference from the design temperature is considered in the calculation of δ_{stator} because a temperature lower than the design temperature is not detrimental to the stator blade. Both positive and negative differences from design temperature are considered in the calculation of δ_{rotor} because a temperature lower than the design temperature, while not causing harm to the rotor blade, results in a deficiency in the work extracted from the gas stream by the turbine compared with that extracted with proper thermal loading of the turbine.

Units

The U.S. customary system of units was used for primary measurements and calculations. Conversion to SI units (Système International d'Unités) is done for reporting

purposes only. In making the conversion, consideration is given to implied accuracy and may result in rounding off the value expressed in SI units.

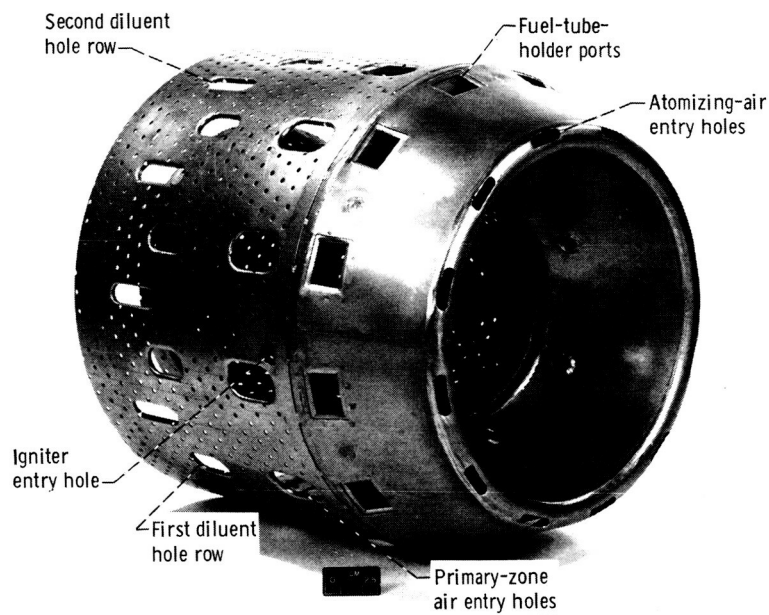
RESULTS AND DISCUSSION

Combustor Development

Development tests. - The first model of the air-atomizing combustor tested is shown in figure 8. In this model, the fuel was atomized by being injected onto a flat atomizer plate and then being stripped off the plate by high-velocity air which flowed over both sides of the plate. The combination fuel tube holder and atomizer plate is shown in figure 9. The atomizer plate was positioned in the firewall as shown in figure 10. The primary-zone air entry holes were somewhat larger in this model than in the final model.

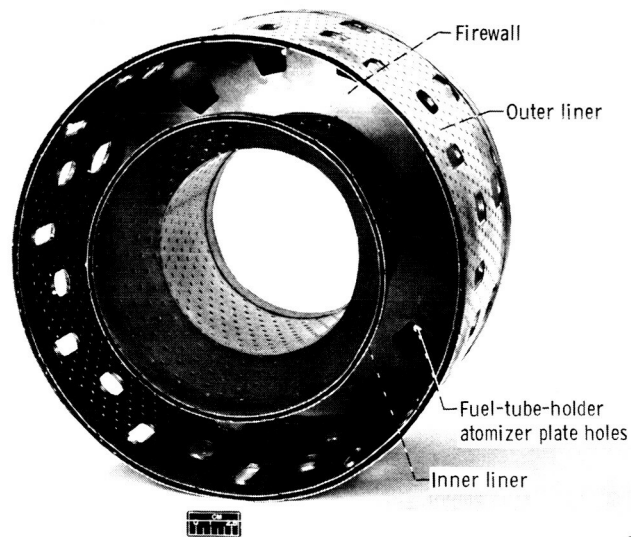
Early test results were encouraging. Combustion efficiency, total-pressure loss, and exit temperature profiles were very good for such an early stage of development. As testing continued at higher fuel flow rates, corresponding to the sea-level-takeoff condition, damage occurred to the combustor firewall. Hot spots appeared near the inner combustor liner, resulting in some holes being burned through the firewall. The entire combustor had been painted with a temperature-sensitive paint prior to testing; and the coloration of this paint led to the conclusion that combustion had been sustained in the snout area of the combustor, upstream of the firewall. It was not clear whether this had taken place after holes had been burned through the firewall, with fuel then recirculating upstream through these holes, or whether fuel had fallen into the snout from the atomizer plate. The latter seemed unlikely because the high-velocity air blowing over both sides of the plate would be expected to carry any splashed fuel through the firewall. It also seemed likely that if some fuel did fall into the snout, a combustible mixture would not be able to accumulate because the continuous supply of new air entering the snout would carry the mixture on through the firewall. The coloration of the temperature-sensitive paint refuted this, however, indicating that the air streams entering the snout probably adhered to the outer wall of the snout, possibly leaving a dead-air zone near the inner snout wall.

A transparent segment of the combustor was constructed (fig. 11). All dimensions were to scale insofar as possible, but the segment was made rectangular to adapt to an existing test facility. Actual fuel tube holders and fuel tubes were used, and the combustor liners were made of the material used for the full annular combustor. All other parts were made of transparent Plexiglass. Airflow through the model was set to simu-



C-69-1982

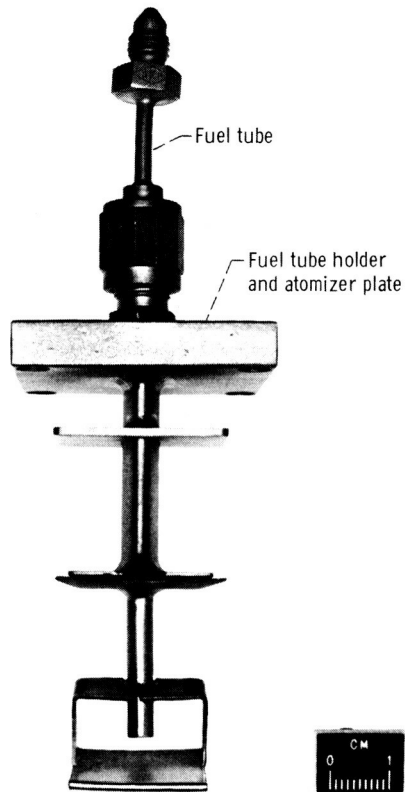
(a) Upstream view.



C-69-1980

(b) Downstream view.

Figure 8. - First model of air-atomizing combustor.



C-69-4120

Figure 9. - Combination fuel tube holder and atomizer plate used in first model of air-atomizing combustor.

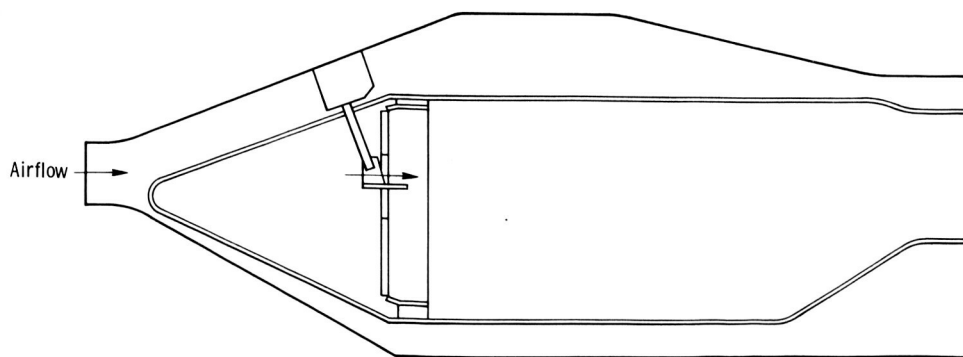
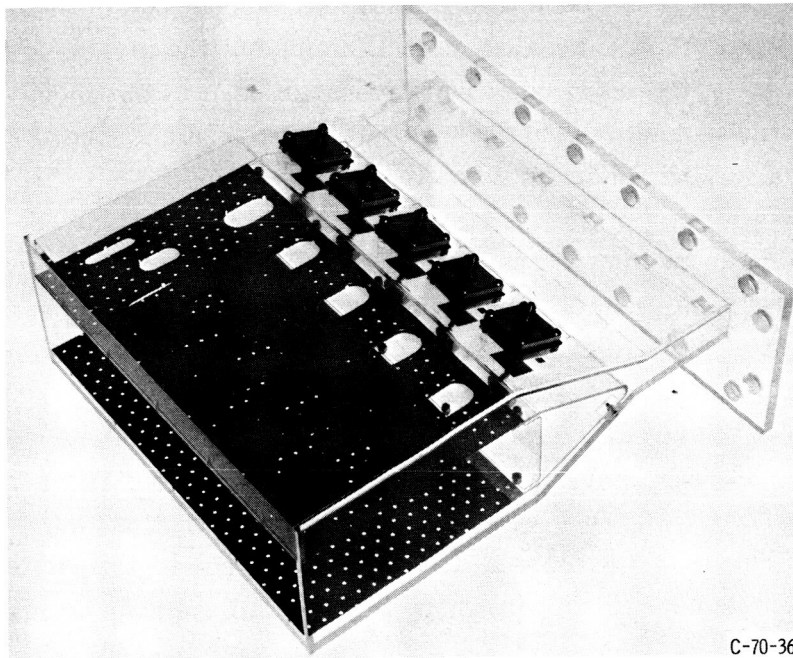
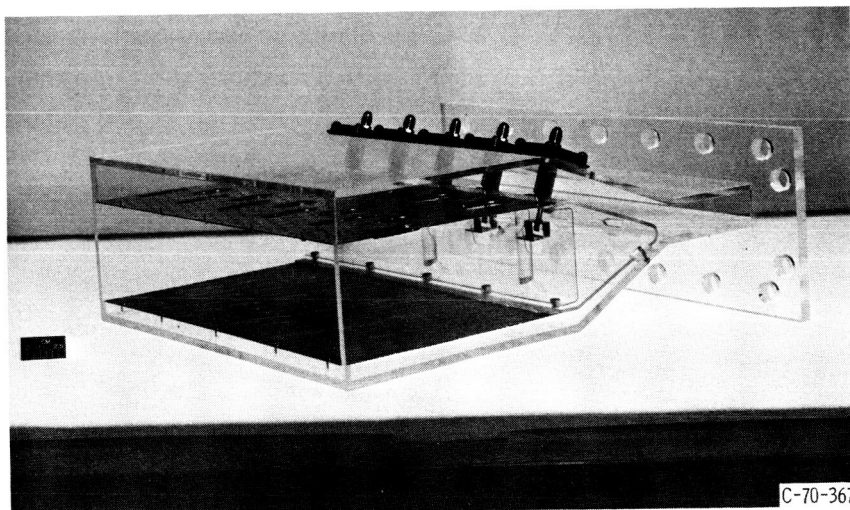


Figure 10. - Positioning of atomizer plate in firewall - first model of air-atomizing combustor.



(a) Top view.



(b) Side view.

Figure 11. - Plexiglass duplication of first model of air-atomizing combustor.

late the reference velocities reached during hot testing, and water was used to simulate the fuel flow. It was very clear from the model tests that

- (1) When low fuel (water) flows were used, none splashed back into the snout
- (2) When higher fuel flows were used, a puddle covered the entire atomizer plate, and some fuel would run off the upstream edge of the plate into the snout
- (3) The air entering the snout adhered to the outer wall of the snout
- (4) There was a stagnant area at the inner wall of the snout, where considerable amounts of fuel would accumulate

Combustor modifications. - Several configurations were tested with the aim of restricting the fuel flow to the downstream side of the firewall, either mechanically, with rectangular chutes running from the snout inlet to the firewall, or by changing the air-flow pattern within the snout to avoid the accumulation of a combustible mixture. Each configuration had its own drawbacks. The best modification turned out to be one of the simplest - the replacement of the atomizer plate by a cylinder welded to the firewall and extending both upstream and downstream. This modification eliminated the firewall burnout problem, and performance was at least as good as that of the original design.

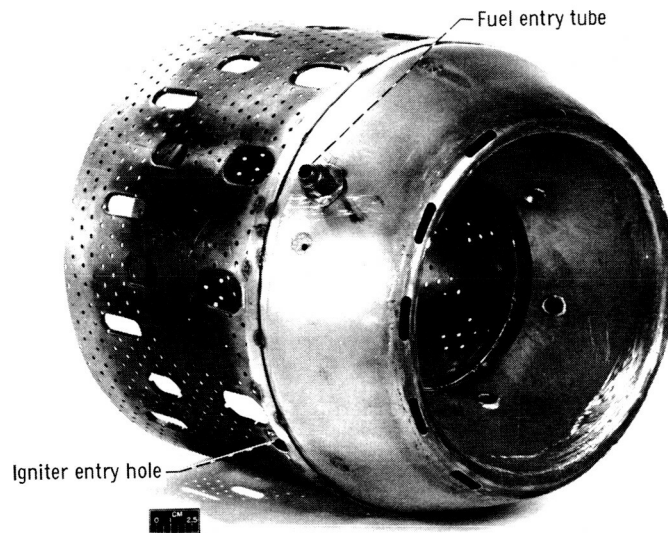
Another modification, a decrease in the size of the primary-zone air entry holes to approximately one-half their original size, made a definite improvement in the combustor exit temperature profiles.

After the development of the air-atomizing combustor had reached its final stage, the simplex nozzle combustor was built, with no changes other than the addition of the simplex fuel nozzles and manifold and the removal of the fuel tube holders and fuel tubes (fig. 12).

Performance Tests

Combustor performance tests were conducted at the nominal test conditions listed in table II. The results of these tests are presented in table III and in the following paragraphs.

Combustion efficiency. - Combustion efficiency data for the air-atomizing combustor are presented in figures 13(a) and (b). Figure 13(a) shows that the combustion efficiency at the cruise design point ($f/a = 0.0116$) is approximately 97 percent, with a rapid dropoff in efficiency with decreasing fuel-air ratio. At the sea-level-takeoff condition, with increased combustor inlet pressure and temperature, combustion efficiency is higher than that at the cruise condition for a given fuel-air ratio, and high efficiencies extend to much lower fuel-air ratios. At the sea-level-takeoff design point ($f/a = 0.0132$), combustion efficiency is approximately 98 percent. Figure 13(b) gives a comparison of the cruise-condition data from figure 13(a) for the 4:1 compression ratio tur-



C-70-1164

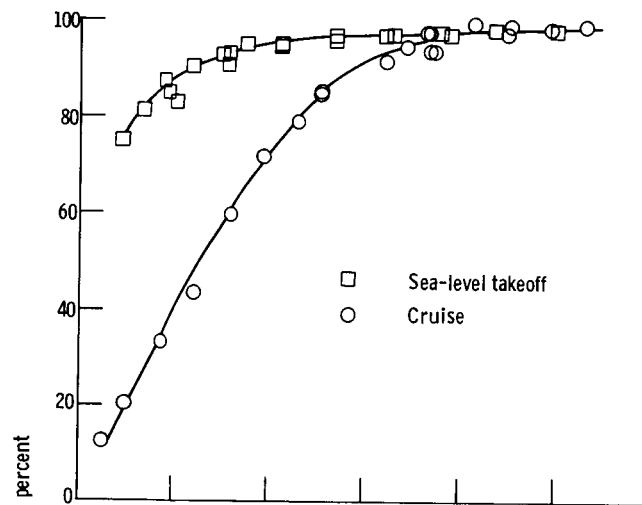
(a) Upstream view.



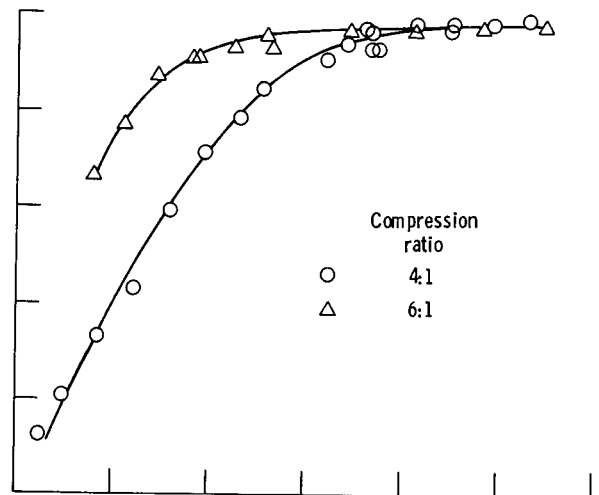
C-70-1165

(b) Downstream view.

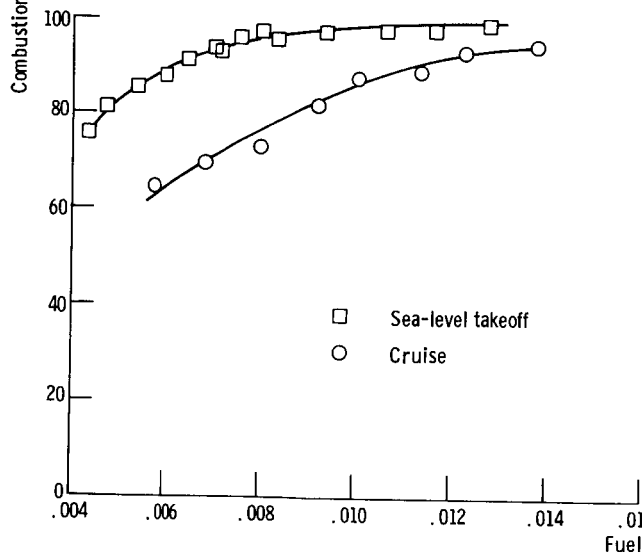
Figure 12. - Simplex nozzle combustor.



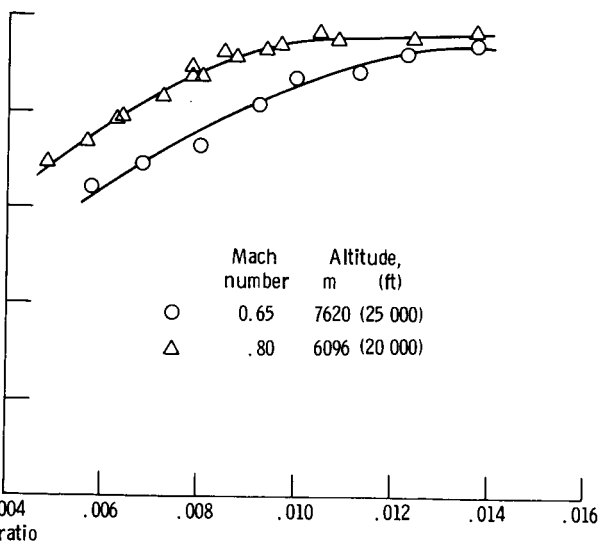
(a) Air-atomizing combustor - sea-level takeoff and cruise at Mach 0.65 and 7620 meters (25 000 ft) altitude.



(b) Air-atomizing combustor - comparison of 4:1 and 6:1 compression ratios at cruise at Mach 0.65 and 7620 meters (25 000 ft) altitude.



(c) Simplex nozzle combustor - sea-level takeoff and cruise at Mach 0.65 and 7620 meters (25 000 ft) altitude.



(d) Simplex nozzle combustor - cruise at Mach 0.65 and 7620 meters (25 000 ft) altitude and at Mach 0.80 and 6096 meters (20 000 ft) altitude.

Figure 13. - Effect of fuel-air ratio on combustion efficiency.

bojet engine and cruise-condition data for a proposed 6:1 compression ratio turbofan engine. Both engines have a cruise design point of Mach 0.65 flight speed at an altitude of 7620 meters (25 000 ft). Performance is improved markedly at the higher combustor inlet temperature and pressure resulting from the 6:1 compression ratio. Design-point ($f/a = 0.0133$) efficiency for the 6:1 ratio cruise point is approximately 98 percent.

Combustion efficiency data for the simplex nozzle combustor are presented in figures 13(c) and (d). The cruise and sea-level-takeoff data shown in figure 13(c) are very similar to those of figure 13(a). Cruise design-point combustion efficiency is slightly lower for the simplex nozzle combustor, but this is not considered to be significant, as no development work was done to improve the performance of this combustor. It is considered significant, however, that a combustor utilizing an air-atomizing device gave performance results at least as good as those of a combustor utilizing an established good fuel atomizer, the simplex nozzle. Figure 13(d) compares the cruise-condition data from figure 13(c) for Mach 0.65 flight speed at an altitude of 7620 meters (25 000 ft) with data for Mach 0.80 flight speed at an altitude of 6096 meters (20 000 ft). The latter condition is of interest as a possible missile flight condition. A 4:1 compression ratio applies in both cases. As in the case of the air-atomizing combustor, the increased combustor inlet pressure and temperature resulted in a noticeable improvement in combustion efficiency.

Limited test data at the design condition for sea-level idle are presented in figure 14. For both the air-atomizing combustor and the simplex nozzle combustor, it was not possible to maintain combustion at a fuel-air ratio lower than 0.009. The desired

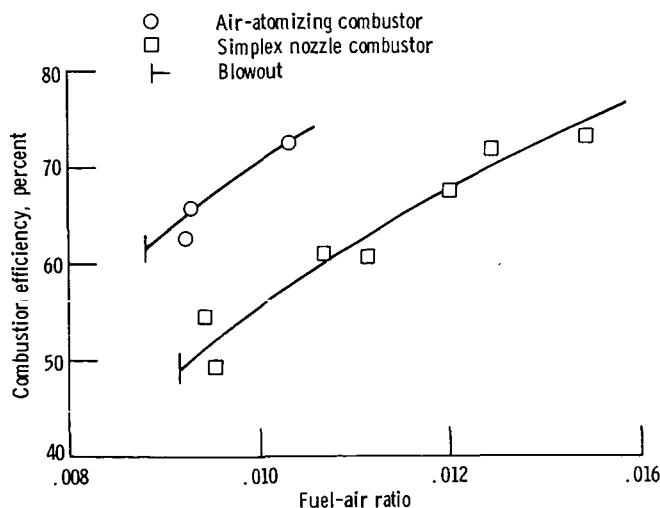


Figure 14. - Effect of fuel-air ratio on combustion efficiency at sea-level idle. Nominal combustor inlet conditions: total pressure, 13.7 N/cm^2 (19.9 psia); temperature, 325 K (125° F).

idle fuel-air ratio is 0.007 at 100 percent combustion efficiency; however, idle speed is maintained by some required combustor exit temperature. In this case, the required exit temperature, specified in table II, is 614 K (645° F). For the air-atomizing combustor, a fuel-air ratio of approximately 0.010 is necessary to maintain the required combustor exit temperature because of low combustion efficiency. At this fuel-air ratio, blowout will not occur; and the combustion efficiency is approximately 71 percent. This low efficiency is not unusual for low-temperature idle conditions. The level of combustion efficiency is somewhat lower in the case of the simplex nozzle combustor. This may be caused by the very low fuel pressure drop across the nozzles at the idle condition.

Total-pressure loss. - The combustor isothermal total-pressure loss $\Delta P/P$ for both the air-atomizing combustor and the simplex nozzle combustor is plotted as a function of the diffuser inlet Mach number in figure 15. At the cruise design point of Mach

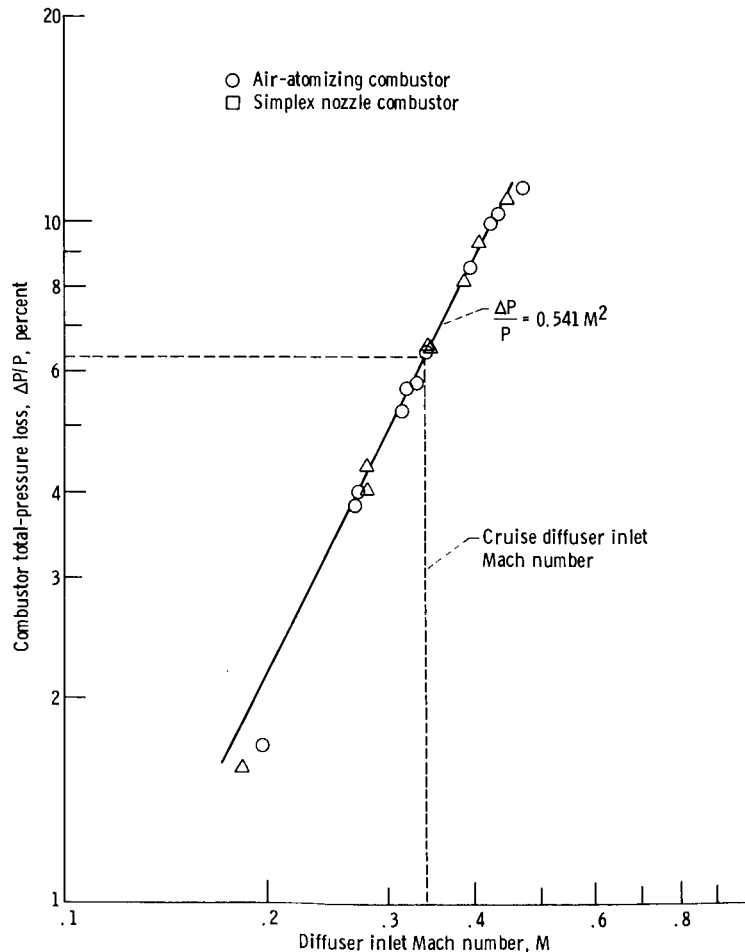


Figure 15. - Variation of combustor isothermal total-pressure loss with diffuser inlet Mach number. Nominal inlet air conditions: total pressure, 20 N/cm² (29 psia); temperature, 38 K (100° F).

0.65 flight speed at an altitude of 7620 meters (25 000 ft), the diffuser inlet Mach number is 0.34, resulting in an isothermal total-pressure loss of approximately 6.3 percent.

Combustor exit temperature profiles. - In the general case, the required average radial temperature profile at the combustor exit plane is determined by limitations on the allowable stresses in the turbine rotor blades and by the requirements for cooling the combustor outlet transition duct. The maximum allowable temperature is usually located at approximately 70 percent of the distance from the blade hub to the blade tip. In the midspan of the blade, the allowable temperature is limited by the creep strength of the blade material. At the hub, the allowable temperature is limited by the fatigue strength of the blade material. At the tip, the allowable temperature is limited by the high-temperature erosion characteristics of the blade material and the fatigue strength at the stator blade hub. No study was made to determine a design radial temperature profile for the low-cost engine. The design profile chosen is typical of those used for turbojet engines of similar size and thrust level.

Comparisons of test data with the design average radial temperature profile are presented in figure 16 for the cruise and sea-level-takeoff conditions for both the air-atomizing combustor and the simplex nozzle combustor. In no case do measured values deviate from design values by more than 25 K (45° F).

The design average circumferential temperature profile at the combustor exit plane is a uniform one, so that no turbine stator blade has a temperature significantly different from the average. Figure 17 presents test results for the cruise and sea-level-takeoff conditions for both the air-atomizing combustor and the simplex nozzle combustor. The profiles shown for the simplex nozzle combustor are slightly better than those for the air-atomizing combustor. A large number of simplex nozzles were flow checked, and a well-matched set of nozzles was chosen for the simplex nozzle combustor. In the case of the air-atomizing combustor, a limited number of fuel tubes were available. The fuel tubes had metering orifices with 0.061-centimeter (0.024-in.) diameter. A small variation in diameter of an orifice this small causes a large increase or decrease in the local fuel flow rate. It is likely that if a quantity of these tubes had been available from which to choose a well-matched set, the exit average circumferential temperature profile of the air-atomizing combustor would have been improved. In any case, the average temperature at any circumferential location seldom deviated from the average exit temperature by more than 50 K (90° F).

Three parameters often used to describe the quality of combustor exit temperature profiles have been defined in the CALCULATIONS section of this report. Values of these parameters, for the same test points for which radial and circumferential profiles have been presented, are given in table IV. The combustor exit temperature pattern factors shown in table IV are unusually good. The worst pattern factor shown, 0.239, means that the maximum individual temperature at the combustor exit was only 122 K (220° F)

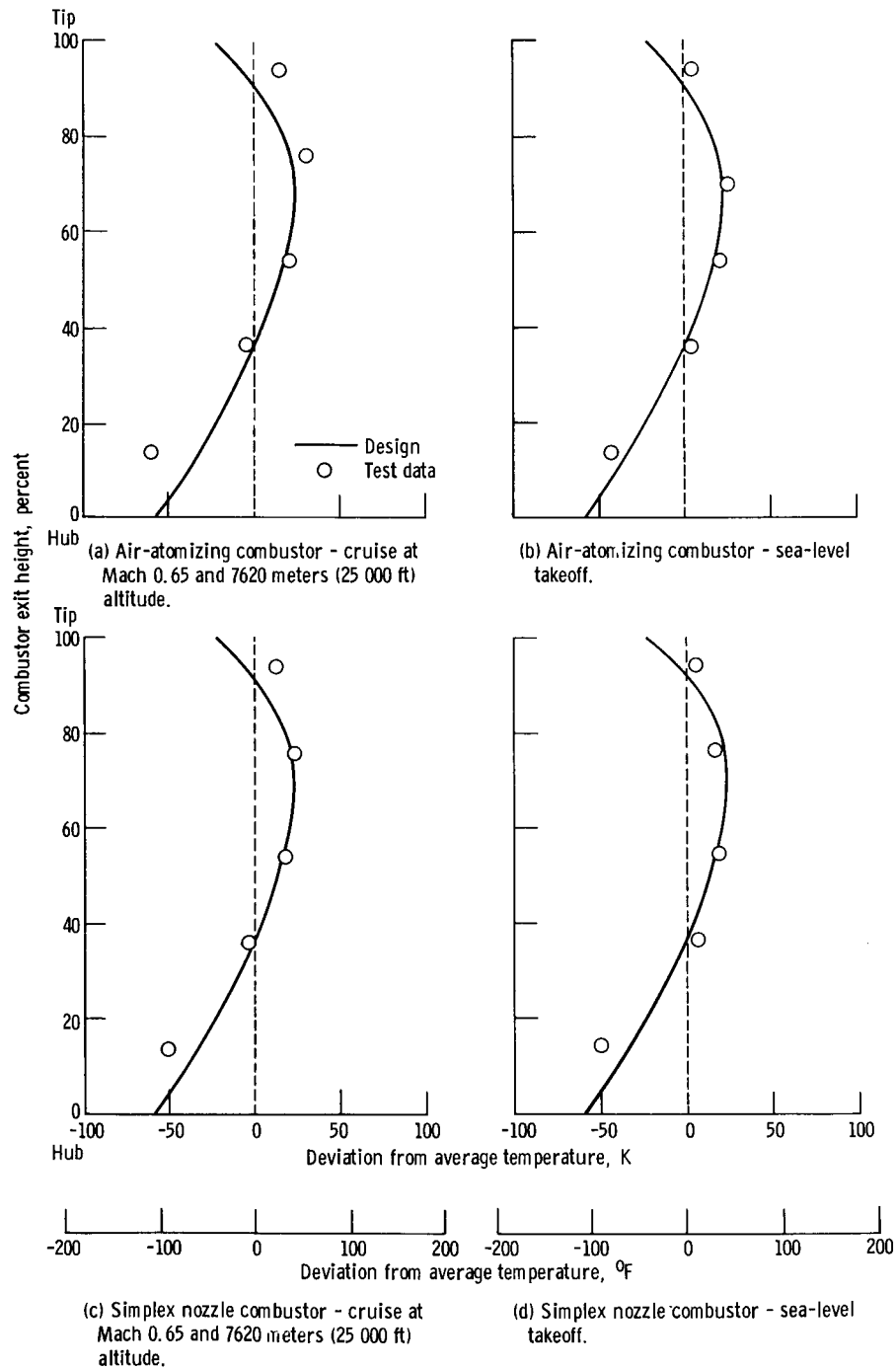


Figure 16. - Combustor average radial exit temperature profile.

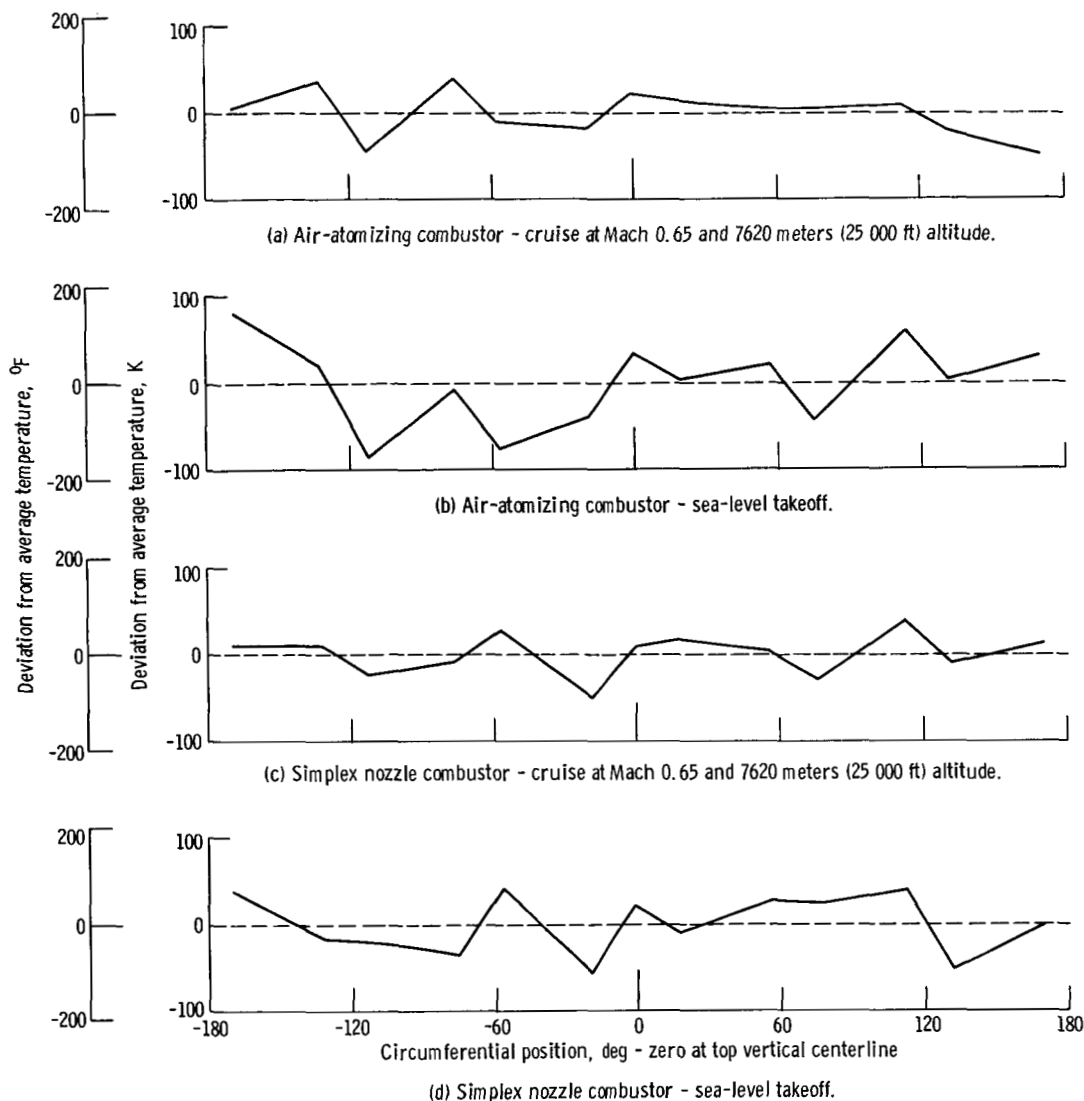


Figure 17. - Combustor average circumferential exit temperature profile.

higher than the average temperature. The lack of significant hot spots should be beneficial in the design of the turbine components, especially the stator.

Altitude ignition tests. - Ignition tests were made in which engine windmilling conditions at various altitudes and flight Mach numbers (tables V and VI) were simulated insofar as combustor airflow rate and inlet total pressure were concerned. Ignition testing was started with estimated values of combustor inlet pressure and temperature; these values were refined later in the test program. Because of this, slight discrepancies arise between tables V and VI at a few points. Combustor inlet total temperature at altitude could not be simulated because a refrigerated air supply was not available.

Air at ambient temperature, approximately 305 K (90° F), was used. The results of these tests are presented in tables VII and VIII.

Figure 18 presents the ignition data in terms of the fuel-air ratio required for ignition as a function of the combustor inlet total pressure. Two other parameters usually used to correlate ignition data - combustor inlet temperature and combustor reference velocity - were not used. The combustor inlet temperature did not vary enough to be a factor. The combustor reference velocity did not appear to have any effect while varying from 15.8 to 28.0 meters per second (51.7 to 92.0 ft/sec); however, two data points for the air-atomizing combustor at an altitude of 3048 meters (10 000 ft) and flight Mach numbers of 0.30 and 0.40 were exceptions. One data point, where the combustor reference velocity is 15.5 meters per second (50.9 ft/sec), departs slightly from the other data. The other data point, where the combustor reference velocity is 11.6 meters per second (38.2 ft/sec), departs significantly from the other data, which suggests the possibility that this air velocity is below that required to produce satisfactory fuel atomization.

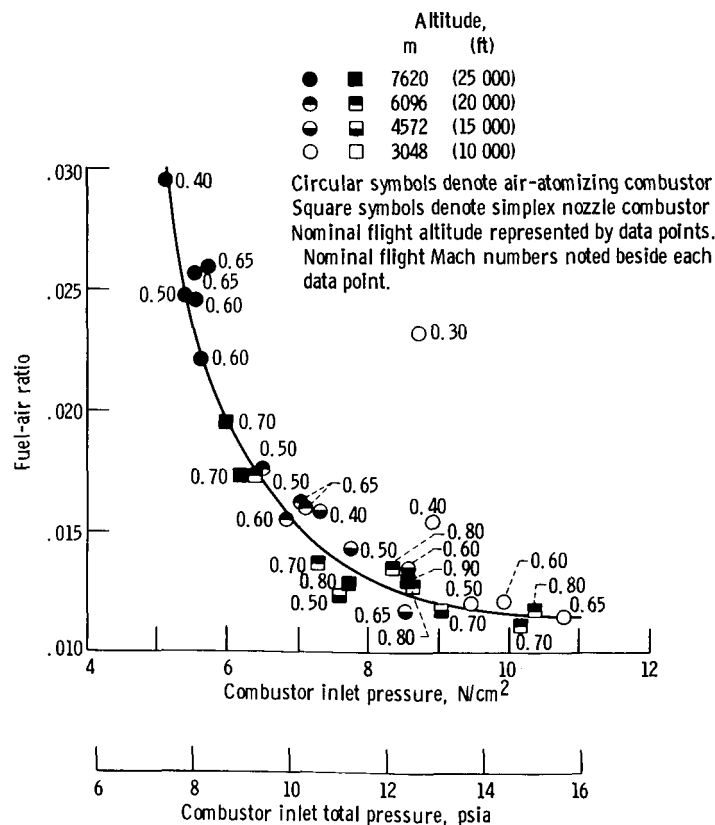


Figure 18. - Variation of fuel-air ratio required for ignition with combustor inlet total pressure. Nominal combustor inlet total temperature, 305 K (90° F).

Because the low-cost engine is designed to operate at moderate turbine inlet temperatures, the allowable fuel-air ratio for ignition must be limited to a relatively low value. The maximum design temperature is that obtained at the sea-level-takeoff condition - 964 K (1275⁰ F). If it is assumed that the combustor, upon ignition, will operate at 85 percent efficiency or less, a fuel-air ratio of approximately 0.020 may be used for ignition without the combustor exit temperature exceeding 964 K (1275⁰ F). Figure 18 shows that a fuel-air ratio of 0.020 will allow ignition at a combustor inlet total pressure of approximately 6.0 N/cm² (8.7 psia). Referring to table V, ignition would then be possible at an altitude of 4572 meters (15 000 ft) at all flight Mach numbers and at 6096 meters (20 000 ft) at flight Mach numbers of 0.40 and higher; however, the lower combustor inlet temperatures at actual flight conditions (table V) can be expected to adversely affect ignition capability.

Durability. - A limited endurance test of three consecutive 1 hour runs at the cruise condition with short cooldown periods between runs produced no damage in the air-atomizing combustor. A 1/2-hour run at the sea-level-takeoff condition caused damage in the form of nibbling away of the upstream edges of the firewall cylinders and some burning away of the firewall. However, many sea-level-takeoff test runs of several minutes duration, a more realistic time during which full power might be applied, did not produce damage at the same test conditions.

Six thermocouples were fixed to the simulated engine shaft. None of the thermocouples had a reading exceeding 533 K (500⁰ F) at any test condition, so that durability of the engine rotating shaft is not endangered by the elimination of the inner combustor housing wall.

Smoke formation and exhaust emissions. - Very limited data indicated that smoke formation and exhaust emissions may be above levels acceptable for commercial aircraft. No effort was made to improve the levels of smoke formation or exhaust emission. It is likely that established techniques, such as using a leaner fuel-air ratio in the combustor primary zone, can reduce the amount of smoke formation. Possible adverse effects of such techniques on altitude ignition capability would have to be evaluated. Gaseous exhaust emission reduction may be a more difficult problem, especially at the sea-level-idle design point. Here severe operating conditions result in low combustion efficiencies.

SUMMARY OF RESULTS

A combustor suitable for use in a low-cost turbojet engine for commercial light aircraft was tested with ASTM A-1 fuel. The final air-atomizing combustor configuration produced the following results:

1. Combustion efficiency was approximately 97 percent at the cruise design point and 98 percent at the sea-level-takeoff design point.

2. Combustor isothermal pressure loss was 6.3 percent at the cruise condition diffuser inlet Mach number of 0.34.

3. Combustor exit radial temperature profiles were in very good agreement with the design profile at both cruise and sea-level-takeoff conditions, with no experimental radial average temperature differing from the design temperature by more than 25 K (45° F).

4. Combustor exit circumferential temperature profiles were satisfactory, with only a few experimental circumferential average temperatures differing from the combustor exit average temperature by as much as 50 K (90° F), and none by as much as 100 K (180° F).

5. Temperature profile quality parameters were very good. For the cruise condition and the sea-level-takeoff condition, respectively, the pattern factor $\bar{\delta}$ was 0.208 and 0.239, δ_{stator} was 0.189 and 0.225, and δ_{rotor} was -0.066 and 0.027.

6. The fuel-air ratio required for ignition was satisfactory at ambient temperature and combustor inlet total pressures as low as 6.0 newtons per square centimeter (8.7 psia). Below this pressure, the fuel-air ratio required for ignition could result in a combustor temperature exceeding the design temperature, at least momentarily, until the compressor would be brought up to speed.

7. Limited endurance testing of 3 consecutive hours at the cruise design condition had no harmful effects on the combustor. A 1/2-hour test at the sea-level-takeoff design condition caused some damage in the form of nibbling away of the upstream edges of the firewall cylinders and some burning away of the firewall. However, many test runs of several minutes duration, a more realistic time during which full power might be applied, did not produce damage at the same sea-level-takeoff conditions.

8. The combustor with air-atomizing devices generally produced results nearly identical with those of a second combustor which used simplex fuel nozzles in place of the air-atomizing devices.

Lewis Research Center,
National Aeronautics and Space Administration,
Cleveland, Ohio, October 13, 1971,
132-15.

APPENDIX A

TEST FACILITY

Testing of the combustor described in this report was conducted in a closed-duct test facility in the Engine Research Building of the Lewis Research Center. A sketch of this facility is shown in figure 19.

A heat exchanger, utilizing the exhaust gases of up to four J-47 combustor cans as a heat source, heated the combustion air to the required combustor inlet temperatures without vitiation. Only a portion of the combustion air passed through the heat exchanger so that a higher fuel-air ratio could be maintained in the J-47 combustor cans, allowing them to operate efficiently. The remaining combustion air bypassed the heat exchanger and mixed with the heated air to provide the desired combustor inlet temperatures.

A large plenum chamber preceding the test section ensured good mixing and temperature uniformity through the use of punched-plate baffles. A bellmouth provided a smooth transition to the test section.

The hot exhaust gases from the combustor were cooled before entering the facility exhaust ducting by a water spray section.

Airflow rates and combustor pressures were regulated by remotely controlled valves upstream and downstream of the test section.

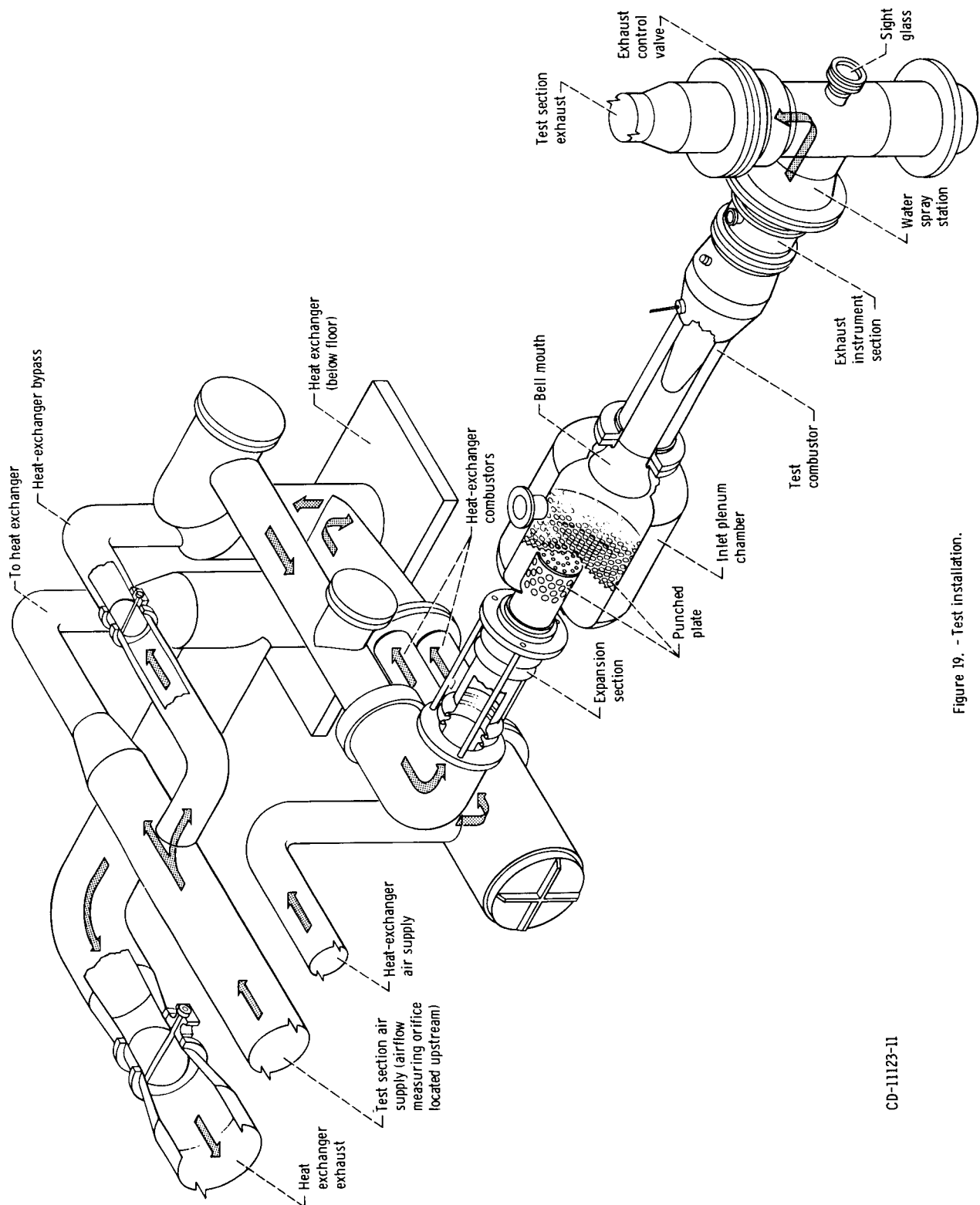


Figure 19. - Test installation.

CD-11123-11

APPENDIX B

INSTRUMENTATION

Test data required to determine combustor performance were recorded at the test facility on punched paper tape. The data were subsequently transferred from the paper tape to a magnetic tape and processed through a digital computer to provide combustor performance results. Control room indicating and recording instrumentation was used to set the test conditions and to monitor the condition of the test section and the test facility. Pressures were measured by strain-gage-type transducers and manometers. Temperatures were measured by iron-constantan and Chromel-Alumel thermocouples of the unshielded wedge type (ref. 10, type 5).

Airflow rates were measured by square-edged orifice plates installed in accordance with ASME specifications. ASTM A-1 fuel-flow rates were measured by turbine flowmeters.

Combustor inlet total temperature was measured by six equally spaced Chromel-Alumel thermocouples located near the upstream flange of the combustor housing (fig. 20, plane A-A). Inlet air total pressure was measured by six equally spaced, five-point, total-pressure rakes at the diffuser inlet (fig. 20, plane B-B). At the same location, static pressures at the diffuser inlet were measured by wall static-pressure taps, with six on the outer annulus wall and three on the inner annulus wall.

Combustor exit total temperature was measured by 13 five-point, Chromel-Alumel, thermocouple rakes, spaced as shown in figure 21 and located at the combustor exit

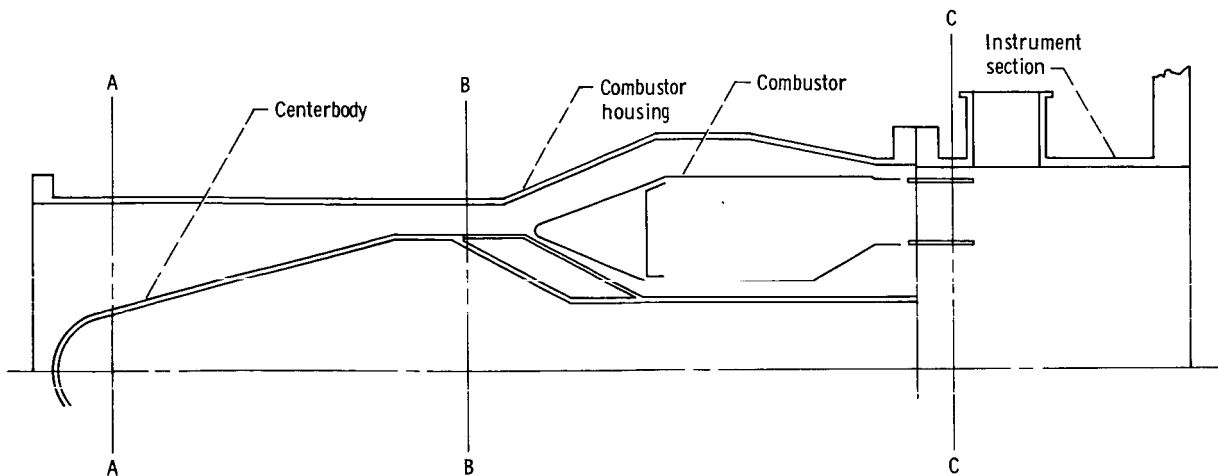


Figure 20. - Schematic drawing of combustor housing and instrument section showing location of instrument planes.

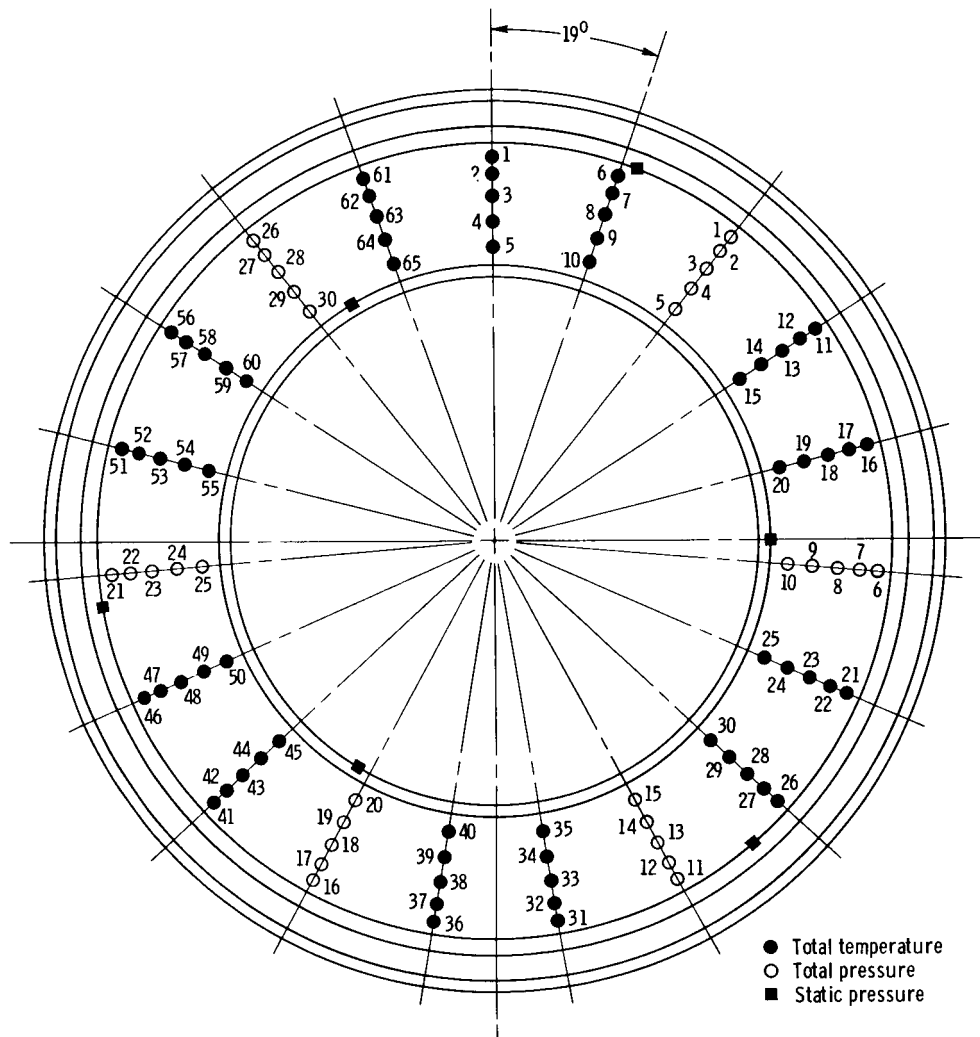


Figure 21. - Combustor exit instrumentation plane, looking downstream, showing locations of combustor exit total-temperature probes, combustor exit total-pressure probes, and combustor exit static-pressure taps.

(fig. 20, plane C-C). At the same location, combustor exit total pressure was measured by six, five-point, total-pressure rakes, spaced as shown in figure 21. Static pressure at the combustor exit was measured by wall static-pressure taps, with three on the outer annulus wall and three on the inner annulus wall.

Six Chromel-Alumel thermocouples were fixed to the inner combustor housing wall, which simulates the engine rotating shaft.

REFERENCES

1. Anon.: Aircraft Propulsion. NASA SP-259, 1971.
2. Roelke, Richard J.; and Stewart, Warner L.: Turbojet and Turbofan Cycle Considerations and Engine Configurations for Application in Lightweight Aircraft. NASA TM X-1624, 1968.
3. Dugan, James F., Jr.: Theoretical Performance of Turbojet Engine for Light Subsonic Aircraft. NASA TM X-52538, 1969.
4. Norgren, Carl T.: Design and Performance of an Experimental Annular Turbojet Combustor with High-Velocity-Air Admission Through One Wall. NASA Memo 12-28-58E, 1958.
5. Humenik, Francis M.: Performance of a Short-Length Turbojet Combustor Insensitive to Radial Distortion of Inlet Airflow. NASA TN D-5570, 1970.
6. Norgren, Carl T.; and Childs, J. Howard: Effect of Liner Air-Entry Holes, Fuel State, and Combustor Size on Performance of an Annular Turbojet Combustor at Low Pressures and High Air-Flow Rates. NACA RM E52J09, 1953.
7. Goldstein, R. J.; Eckert, E. R. G.; and Ramsey, J. W.: Film Cooling with Injection Through Holes - Adiabatic Wall Temperatures Downstream of a Circular Hole. Paper 68-GT-19, ASME, Mar. 1968.
8. Fear, James S.: Preliminary Evaluation of a Perforated Sheet Film-Cooled Liner in a Turbojet Combustor. NASA TM X-52705, 1969.
9. Biaglow, James A.: Preliminary Tests of a Gas Turbine Combustor with an Air Atomizing Fuel Injector System. NASA TM X-52688, 1969.
10. Glawe, George E.; Simmons, Frederick S.; and Stickney, Truman M.: Radiation and Recovery Corrections and Time Constants of Several Chromel-Alumel Thermocouples Probes in High-Temperature, High-Velocity Gas Streams. NACA TN 3766, 1956.

TABLE I. - COMBUSTOR DIMENSIONS - FINAL DESIGN

Length, cm (in.):	
Compressor exit to turbine inlet	35.79 (14.09)
Firewall to turbine inlet	23.50 (9.25)
Diameter, cm (in.):	
Inlet, outside	29.220 (11.504)
Inlet, inside	24.133 (9.501)
Exit, outside	32.680 (12.866)
Exit, inside	22.108 (8.704)
Combustor liner volume, m ³ (ft ³)	0.0159 (0.561)
Combustor reference area, cm ² (in. ²)	1144.58 (177.41)
Diffuser inlet area, cm ² (in. ²)	214.45 (33.24)
Open hole area, cm ² (in. ²):	
Atomizing-air holes	23.23 (3.60)
Primary-zone holes	70.84 (10.98)
First diluent hole row	76.00 (11.78)
Second diluent hole row	68.19 (10.57)
Cooling holes in perforated sheet	162.26 (25.15)
Firewall cylinder openings ^a	52.68 (8.17)
Swirler openings ^b	65.76 (10.19)
Ratio, length to height at reference plane	2.58

^aPertains to air-atomizing combustor only.^bPertains to simplex nozzle combustor only.

TABLE II. - NOMINAL COMBUSTOR TEST CONDITIONS

Test point	Combustor	Design point	Compression ratio	Flight altitude		Combustor inlet total pressure		Combustor inlet total temperature		Airflow rate		Combustor exit total temperature		Reference velocity		Fuel-air ratio at 100 percent combustion efficiency
				m	ft	N/cm ²	psia	K	°F	kg/sec	lb/sec	K	°F	m/sec	ft/sec	
1	Air atomizing and simplex nozzle	Mach 0.65 cruise	4:1	7620	25 000	19.8	28.7	406	271	4.51	9.94	867	1100	23.1	75.8	0.0116
2		Sea-level takeoff	4:1	0	0	38.5	55.8	452	353	8.32	18.35	964	1275	24.5	80.3	0.0132
3	Air atomizing and simplex nozzle	Idle	4:1	0	0	13.7	19.9	325	125	2.92	6.44	614	645	17.6	57.6	0.0070
4	Air atomizing	Mach 0.65 cruise	6:1	7620	25 000	30.0	43.5	463	373	6.32	13.94	978	1300	24.4	80.2	0.0133
5	Simplex nozzle	Mach 0.80 cruise	4:1	6096	20 000	28.4	41.2	437	327	6.26	13.80	1089	1500	24.1	79.1	0.0172

TABLE III. - EXPERIMENTAL COMBUSTION EFFICIENCY AND ISOTHERMAL PRESSURE LOSS DATA

Test point (see table II)	Combustor inlet conditions									Combustor operation results						
	Run	Pressure		Temperature		Airflow rate		Reference velocity		Diffuser inlet Mach number	Fuel-air ratio	Exit total temperature		Combustion efficiency, percent	Pressure loss ratio, ΔP/P, percent	ξ
		N/cm	psia	K	°F	kg/sec	lb/sec	m/sec	ft/sec			K	°F			
Test point 2; air-atomizing combustor; fig. 16(a)	001	38.5	55.9	455	359	8.33	18.37	24.7	81.2	0.339	0.01399	979	1303	98.1	6.98	0.235
	002	39.0	56.6			8.33	18.37	24.4	80.1	.335	.01273	934	1222	97.8	6.39	.239
	003	38.2	55.4			8.29	18.28	24.8	81.4	.343	.01179	899	1159	97.3	6.69	.272
	004	38.7	56.1			8.32	18.35	25.1	82.2	.344	.01162	893	1148	97.6	6.59	.219
	005	38.7	56.1	456	360	8.30	18.29	24.5	80.4	.338	.01060	856	1081	96.8	6.44	.231
	006	38.0	55.1	454	358	8.32	18.34	25.0	82.0	.347	.01041	847	1064	96.4	6.94	.195
	007	39.1	56.7	456	360	8.28	18.26	24.2	79.5	.334	.00939	812	1001	96.5	6.10	.208
	008	38.5	55.8	454	358	8.33	18.36	24.7	81.2	.342	.00938	809	996	96.0	6.76	.199
	009	37.9	54.9	455	359	8.32	18.34	25.1	82.4	.348	.00825	767	921	95.5	6.72	.203
	010	38.7	56.2	455	359	8.34	18.38	25.0	82.1	.345	.00823	763	913	94.5	6.48	.221
	011	37.9	54.9	456	360	8.28	18.25	25.0	82.0	.347	.00759	743	878	95.4	6.80	.234
	012	39.0	56.6	456	360	8.31	18.32	24.4	79.9	.335	.00719	723	842	93.4	6.04	.210
	013	38.9	56.4	455	359	8.31	18.32	24.4	80.1	.336	.00717	714	826	90.8	6.42	.216
	014	38.6	56.0	456	360	8.27	18.23	24.5	80.5	.339	.00702	716	829	92.9	6.41	.246
	015	38.1	55.2	456	360	8.28	18.25	24.9	81.6	.345	.00643	687	777	90.0	6.44	.274
	016	38.6	56.0	454	358	8.31	18.33	24.6	80.7	.342	.00607	655	719	82.2	6.19	.267
	017	37.9	55.0	456	360	8.32	18.35	25.1	82.3	.349	.00594	658	725	84.9	6.59	.276
	018	39.1	56.7	455	359	8.27	18.23	24.2	79.3	.334	.00575	658	724	87.4	5.80	.300
	019	39.2	56.8	455	359	8.27	18.23	24.1	79.2	.332	.00534	629	672	80.5	5.98	.335
	020	38.7	56.1	455	359	8.27	18.24	24.5	80.3	.338	.00483	601	622	74.6	6.04	.399
Test point 1; air-atomizing combustor; figs. 16(a) and (b)	021	19.8	28.7	415	287	4.44	9.79	23.4	76.9	0.338	0.01461	974	1294	99.6	7.48	0.226
	022	20.0	29.0	416	288	4.45	9.80	23.2	76.1	.333	.01391	944	1240	98.5	7.39	.238
	023	19.9	28.8	415	287		9.82	23.4	76.8	.339	.01301	915	1187	98.9	7.64	.227
	024	19.8	28.7	423	301		9.80	23.8	78.2	.341	.01295	912	1181	97.4	6.87	.235
	025	19.7	28.6	415	287		9.81	23.5	77.1	.339	.01231	891	1144	99.1	7.40	.225
	026	19.4	28.1	422	300	4.45	9.80	24.4	79.9	.352	.01145	841	1054	93.5	7.25	.212
	027	21.2	30.8	407	273	4.48	9.87	21.5	70.6	.310	.01137	827	1029	93.9	5.56	.208
	028	20.0	29.0	415	287	4.45	9.82	23.2	76.1	.336	.01136	847	1065	96.9	7.18	.254
	029	19.9	28.9	415	287	4.45	9.80	23.2	76.3	.336	.01126	845	1061	97.5	7.29	.226
	030	19.5	28.3	423	301	4.45	9.80	24.2	79.3	.347	.01086	826	1026	94.4	7.05	.212
	031	19.6	28.4	423	301	4.44	9.78	24.0	78.9	.344	.01042	797	974	91.1	6.76	.208
	032	19.5	28.3			4.45	9.82	24.2	79.4	.351	.00912	730	854	84.9	6.86	.264
	033	20.0	29.0			4.45	9.80	23.6	77.4	.337	.00862	694	790	79.0	6.43	.304
	034	19.9	28.8			4.46	9.83	23.8	78.2	.344	.00791	650	710	71.7	6.35	.379
	035	20.1	29.1			4.46	9.83	23.6	77.4	.336	.00720	595	611	59.5	5.97	.521
	036	20.0	29.0	423	301	4.46	9.84	23.7	77.7	.339	.00643	536	504	43.4	6.10	.954
	037	20.0	29.0			4.47	9.86	23.7	77.9	.336	.00569	499	439	33.2	6.13	1.305
	038	19.9	28.8			4.48	9.87	24.0	78.7	.343	.00498	464	376	20.4	5.97	2.148
	039	19.7	28.6			4.48	9.87	24.1	79.2	.345	.00447	445	341	12.3	6.35	3.161
Test point 4; air-atomizing combustor; fig. 16(b)	040	29.4	42.7	462	371	6.40	14.10	25.2	82.8	0.347	0.01497	1020	1376	98.4	7.14	0.206
	041	30.1	43.7	462	371		14.12	24.6	80.8	.336	.01370	974	1294	98.0	6.60	.202
	042	30.0	43.5	464	376		14.11	24.9	81.7	.342	.01224	925	1205	97.7	6.72	.185
	043	29.4	42.6	464	375		14.11	25.4	83.2	.347	.01092	875	1115	96.9	6.95	.175
	044	29.4	42.6	466	378	6.39	14.08	25.7	84.3	.351	.00930	812	1002	95.0	6.78	.189
	045	29.7	43.1	461	369	6.38	14.07	24.9	81.6	.342	.00920	808	995	96.0	6.61	.174
	046	29.7	43.1	462	371	6.40	14.10	25.0	81.9	.341	.00850	776	937	93.8	6.50	.186
	047	30.0	43.5	465	377	6.39	14.09	24.9	81.6	.341	.00779	746	882	90.9	6.34	.201
	048	29.9	43.4	462	371	6.40	14.12	24.8	81.4	.340	.00768	739	871	91.0	6.29	.199
	049	29.4	42.7	462	371	6.40	14.12	25.2	82.7	.346	.00688	700	800	86.8	6.53	.213
	050	30.1	43.7	461	369	6.40	14.12	24.6	80.7	.336	.00623	653	715	77.0	6.02	.263
	051	29.6	43.0	462	371	6.40	14.11	25.0	82.0	.346	.00560	611	640	66.3	6.67	.334

TABLE III. - Continued. EXPERIMENTAL COMBUSTION EFFICIENCY AND ISOTHERMAL PRESSURE LOSS DATA

Test point (see table II)	Run	Combustor inlet conditions								Combustor operation results						
		Pressure		Temperature		Airflow rate		Reference velocity		Diffuser inlet Mach number	Fuel-air ratio	Exit total temperature		Combustion efficiency, percent	Pressure loss ratio, ΔP/P, percent	η
		N/cm	psia	K	°F	kg/sec	lb/sec	m/sec	ft/sec			K	°F			
Test point 2; simplex nozzle com- bustor; fig. 16(c)	052	37.2	54.0	459	366	8.27	18.24	25.6	84.1	0.352	0.01278	947 1245	99.3	6.81	0.133	
	053	38.5	55.9	457	363	8.17	18.02	24.3	79.8	.333	.01167	898 1157	97.7	6.39	.129	
	054	38.9	56.4		362	8.16	17.99	24.1	79.0	.331	.01063	859 1086	97.1	6.20	.120	
	055	38.8	56.3	↓	362	8.19	18.05	24.2	79.5	.333	.00938	812 1001	96.3	6.13	.123	
	056	38.2	55.4	↓	362	8.18	18.03	24.6	80.6	.339	.00834	771 928	95.2	6.60	.166	
	057	38.4	55.7	457	362	8.21	18.09	24.5	80.4	.337	.00800	762 912	96.4	6.46	.160	
	058	38.9	56.4	↓	362	8.21	18.10	24.2	79.4	.333	.00757	744 880	95.7	6.21	.161	
	059	38.5	55.9		363	8.17	18.02	24.4	79.9	.334	.00716	723 841	93.1	6.36	.208	
	060	38.6	56.0	↓	363	8.21	18.09	24.4	80.1	.335	.00699	718 833	93.5	6.39	.219	
	061	38.5	55.8	457	362	8.23	18.14	24.6	80.6	.338	.00647	693 788	91.3	6.31	.216	
	062	39.0	56.6		362	8.17	18.01	24.0	78.9	.329	.00601	669 744	87.8	5.94	.283	
	063	38.6	56.0		362	8.20	18.08	24.4	79.9	.334	.00539	642 696	85.3	6.29	.367	
	064	38.6	56.0	↓	363	8.21	18.09	24.4	80.1	.336	.00475	612 642	80.7	6.32	.355	
	065	38.6	56.0	↓	363	8.19	18.05	24.3	79.8	.334	.00440	592 606	75.6	6.18	.387	
Test point 1; simplex nozzle com- bustor; figs. 16(c) and (d)	066	20.6	29.9	413	284	4.52	9.96	22.8	74.8	0.327	0.01380	916 1188	94.1	6.35	0.185	
	067	20.1	29.2	414	285	4.54	10.00	23.5	77.0	.339	.01228	857 1082	92.5	6.65	.165	
	068	19.7	28.6	413	284	4.49	9.89	23.6	77.4	.341	.01134	809 996	88.8	6.72	.169	
	069	21.4	31.0	414	285	4.56	10.05	22.1	72.6	.314	.01013	762 911	86.9	5.59	.162	
	070	20.6	29.9	414	285	4.50	9.92	22.6	74.3	.324	.00925	714 826	81.7	6.05	.183	
	071	20.1	29.2	414	285	4.53	9.99	23.4	76.7	.335	.00801	649 708	73.0	6.20	.237	
	072	19.4	28.1	414	285	4.45	9.81	23.9	78.3	.346	.00686	607 632	69.4	6.62	.330	
073	21.0	30.5	414	286	4.49	9.89	22.2	72.9	.316	.00579	565 557	64.1	5.28	.364		
Test point 5; simplex nozzle com- bustor; fig. 16(d)	074	28.2	40.9	438	328	6.29	13.87	24.6	80.6	0.347	0.01377	947 1245	96.3	7.21	0.143	
	075	28.5	41.3	438	328	6.24	13.75	24.1	79.1	.338	.01244	898 1157	95.5	6.81	.146	
	076	28.0	40.6	436	327	6.29	13.87	24.7	81.0	.349	.01089	844 1059	95.4	7.16	.156	
	077	28.3	41.0	438	328	6.28	13.84	24.4	80.1	.344	.01052	834 1042	96.1	6.83	.146	
	078	27.8	40.3	438	328	6.29	13.86	24.9	81.6	.352	.00970	797 975	94.0	6.93	.134	
	079	28.5	41.3	436	327	6.30	13.90	24.4	79.9	.343	.00940	783 950	93.2	6.85	.150	
	080	29.2	42.3	438	328	6.28	13.85	23.7	77.8	.332	.00878	757 902	91.6	6.11	.150	
	081	28.5	41.4	438	329	6.28	13.85	24.2	79.4	.340	.00858	752 894	92.2	6.73	.159	
	082	28.5	41.3	436	327	6.30	13.90	24.3	79.7	.342	.00801	716 828	87.1	6.63	.189	
	083	29.5	42.8	439	330	6.14	13.53	22.9	75.2	.317	.00788	714 826	87.7	5.53	.204	
	084	28.8	41.8	438	329	6.31	13.91	24.1	79.2	.337	.00783	717 830	89.2	6.25	.190	
	085	28.3	41.0	438	329	6.29	13.86	24.5	80.3	.346	.00726	679 762	82.8	6.76	.271	
	086	28.7	41.6	438	328	6.29	13.86	24.1	79.2	.338	.00642	642 695	78.6	6.37	.305	
	087	28.5	41.3	436	327	6.52	14.38	25.2	82.6	.359	.00631	637 687	78.5	7.07	.371	
	088	28.3	41.0	438	329	6.31	13.91	24.5	80.5	.345	.00567	607 633	73.8	6.70	.342	
	089	28.5	41.4	438	329	6.28	13.84	24.2	79.4	.339	.00484	575 575	69.4	6.73	.390	
Test point 3; air-atomizing and simplex nozzle com- bustors; fig. 17	090	13.7	19.8	328	130	2.79	6.15	16.9	55.3	0.263	0.01031	629 672	72.4	4.70	0.361	
	091	13.9	20.2	328	130	2.78	6.13	16.4	53.8	.255	.00929	578 580	65.8	4.23	.279	
	092	14.1	20.4	327	129	2.80	6.17	16.3	53.6	.256	.00921	561 549	62.5	4.20	.329	
	093	13.8	20.0	328	130	2.98	6.56	18.0	58.9	.278	.01345	721 837	73.2	5.43	.265	
	094	13.8	20.0	329	132	2.80	6.18	16.8	55.2	.262	.01245	684 772	71.8	4.91	.292	
	095	13.4	19.5	326	127	2.98	6.56	18.1	59.3	.283	.01202	660 728	67.3	5.47	.310	
	096	13.2	19.2	329	133	2.83	6.24	17.6	57.9	.277	.01113	601 621	60.7	5.06	.389	
	097	13.8	20.0	326	127	2.97	6.55	17.7	58.0	.275	.01066	588 598	61.0	4.88	.294	
	098	13.8	20.0	326	127	2.98	6.56	17.7	58.0	.275	.00953	517 470	49.2	4.91	.450	
	099	13.7	19.8	330	134	2.88	6.34	17.4	57.2	.274	.00942	538 508	54.4	4.97	.346	

TABLE III. - Concluded. EXPERIMENTAL COMBUSTION EFFICIENCY AND ISOTHERMAL PRESSURE LOSS DATA

Test point (see table II)	Run	Combustor inlet conditions								Combustor operation results						
		Pressure		Temperature		Airflow rate		Reference velocity		Diffuser inlet Mach number	Fuel-air ratio	Exit total temperature		Combustion efficiency, percent	Pressure loss ratio, $\Delta P/P$, percent	$\bar{\delta}$
		N/cm	psia	K	°F	kg/sec	lb/sec	m/sec	ft/sec			K	°F			
Isothermal total pressure loss at various diffuser inlet Mach numbers; air-atomizing and simplex nozzle com- bustors; fig. 18	100	19.8	28.7	314	106	6.60	14.56	26.4	86.6	0.471	-----	---	----	----	11.76	-----
	101	20.5	29.8	304	88	6.76	14.91	25.2	82.8	.452	-----	---	----	----	10.95	-----
	102	21.1	30.6	302	83	6.83	15.05	24.5	80.5	.437	-----	---	----	----	10.12	-----
	103	19.3	28.0	302	83	6.09	13.43	24.0	78.6	.425	-----	---	----	----	9.86	-----
	104	19.8	28.7	307	93	6.04	13.32	23.5	77.2	.410	-----	---	----	----	9.29	-----
	105	20.4	29.6	316	109	5.97	13.17	23.3	76.3	.396	-----	---	----	----	8.48	-----
	106	20.8	30.2	308	95	6.10	13.45	22.7	74.5	.389	-----	---	----	----	8.15	-----
	107	20.1	29.2	309	96	5.37	11.83	20.7	67.9	.346	-----	---	----	----	6.48	-----
	108	19.9	28.9	308	94	5.28	11.64	20.5	67.3	.343	-----	---	----	----	6.54	-----
	109	20.1	29.2	316	109	5.25	11.57	20.7	67.9	.341	-----	---	----	----	6.42	-----
	110	20.2	29.3	411	279	4.49	9.89	22.9	75.1	.330	-----	---	----	----	5.78	-----
	111	20.4	29.6	413	283	4.40	9.71	22.4	73.4	.320	-----	---	----	----	5.66	-----
	112	21.3	30.9	302	84	5.33	11.76	19.0	62.3	.316	-----	---	----	----	5.25	-----
	113	20.4	29.6	309	96	4.55	10.02	17.3	56.8	.280	-----	---	----	----	4.03	-----
	114	20.2	29.3	308	95	4.50	9.91	17.2	56.4	.279	-----	---	----	----	4.37	-----
	115	20.1	29.1	316	109	4.29	9.46	17.0	55.7	.271	-----	---	----	----	3.99	-----
	116	20.6	29.9	303	85	4.48	9.87	16.5	54.2	.269	-----	---	----	----	3.80	-----
	117	19.4	28.2	316	109	3.09	6.81	12.6	41.4	.196	-----	---	----	----	1.70	-----
118	20.5	29.7	308	95	3.10	6.84	11.7	38.5	.183	-----	---	----	----	1.59	-----	

TABLE IV. - COMBUSTOR EXIT TEMPERATURE

QUALITY PARAMETERS

Design condition	Combustor	$\bar{\delta}$	δ_{stator}	δ_{rotor}
Mach 0.65 cruise	Air atomizing	0.208	0.189	-0.066
Sea-level takeoff	Air atomizing	.239	.225	.027
Mach 0.65 cruise	Simplex nozzle	.169	.180	.050
Sea-level takeoff	Simplex nozzle	.133	.149	-.037

TABLE V. - NOMINAL WINDMILLING COMBUSTOR INLET

CONDITIONS - AIR-ATOMIZING COMBUSTOR

Flight Mach number	Altitude		Airflow rate		Pressure		Temperature	
	m	ft	kg/sec	lb/sec	N/cm ²	psia	K	°F
0.65	7620	25 000	1.87	4.13	5.76	8.35	275	35
.60	↓	↓	1.67	3.68	5.53	8.02	268	23
.50	↓	↓	1.34	2.95	5.14	7.45	258	4
.40	↓	↓	1.04	2.30	4.83	7.01	250	-10
.30	↓	↓	.79	1.74	4.61	6.69	244	-20
.65	6096	20 000	2.27	5.00	7.12	10.32	284	52
.60	↓	↓	2.04	4.49	6.84	9.92	278	40
.50	↓	↓	1.62	3.57	6.36	9.22	267	21
.40	↓	↓	1.24	2.74	5.98	8.68	259	7
.30	↓	↓	.95	2.10	5.71	8.28	254	-3
.65	4572	15 000	2.72	6.00	8.72	12.65	295	71
.60	↓	↓	2.42	5.34	8.30	12.04	289	60
.50	↓	↓	1.95	4.30	7.80	11.31	278	40
.40	↓	↓	1.52	3.34	7.34	10.64	269	25
.30	↓	↓	1.15	2.53	7.00	10.15	264	15
.65	3048	10 000	3.25	7.17	10.65	15.45	304	88
.60	↓	↓	2.93	6.46	10.23	14.83	298	76
.50	↓	↓	2.34	5.15	9.52	13.80	287	56
.40	↓	↓	1.82	4.01	8.96	13.00	279	42
.30	↓	↓	1.37	3.03	8.54	12.39	273	31

TABLE VI. - NOMINAL WINDMILLING COMBUSTOR INLET

CONDITIONS - SIMPLEX NOZZLE COMBUSTOR

Flight Mach number	Altitude		Airflow rate		Pressure		Temperature	
	m	ft	kg/sec	lb/sec	N/cm ²	psia	K	°F
0.90	7620	25 000	3.12	6.88	8.29	12.02	314	105
.80	7620	25 000	2.53	5.57	6.77	9.82	296	73
.70	7620	25 000	2.07	4.57	5.90	8.55	281	46
.90	6096	20 000	3.75	8.27	10.18	14.76	324	124
.80	↓	↓	3.06	6.75	8.38	12.15	306	90
.70	↓	↓	2.49	5.50	7.24	10.50	291	64
.50	↓	↓	1.62	3.57	5.86	8.50	268	22
.90	4572	15 000	4.51	9.95	12.48	18.10	340	152
.80	↓	↓	3.69	8.13	10.29	14.92	318	112
.70	↓	↓	3.03	6.68	8.96	13.00	302	84
.50	↓	↓	1.95	4.29	7.31	10.60	278	40
.80	3048	10 000	4.41	9.72	12.55	18.20	328	130
.70	3048	10 000	3.60	7.94	10.62	15.40	311	100
.50	3048	10 000	2.33	5.14	8.83	12.80	287	56

TABLE VII. - EXPERIMENTAL WINDMILLING IGNITION DATA - AIR-ATOMIZING COMBUSTOR

Nominal flight conditions				Combustor inlet conditions								Combustor operation results			
Run	Flight Mach number	Altitude		Airflow rate		Pressure		Temperature		Reference velocity		Fuel-air ratio required	Combustion efficiency, percent	Temperature rise after ignition	
		m	ft	kg/sec	lb/sec	N/cm ²	psia	K	°F	m/sec	ft/sec			K	°F
119	0.65	7620	25 000	1.85	4.07	5.73	8.31	308	94	25.0	81.9	.0259	56.7	543	977
120	.65	↓	↓	1.93	4.26	5.54	8.04	299	78	26.2	86.1	.0256	52.2	496	892
121	.60	↓	↓	1.71	3.78	5.63	8.16	308	95	23.6	77.6	.0221	54.8	457	822
122	.60	↓	↓	1.73	3.81	5.56	8.07	302	83	23.5	77.2	.0245	62.7	573	1031
123	.50	↓	↓	1.36	3.00	5.41	7.85	307	93	19.3	63.4	.0247	63.4	582	1047
124	.40	↓	↓	1.05	2.31	5.12	7.42	305	89	15.8	51.7	.0295	63.3	677	1218
125	.65	6096	20 000	2.27	5.00	7.11	10.32	304	88	24.4	80.1	.0160	64.8	537	966
126	.65	↓	↓	2.31	5.10	7.05	10.23	303	85	25.0	82.0	.0162	63.8	405	729
127	.60	↓	↓	2.00	4.42	6.85	9.93	306	90	22.5	73.7	.0155	63.6	386	694
128	.50	↓	↓	1.70	3.75	6.52	9.45	297	74	19.5	63.9	.0176	60.2	412	741
129	.65	4572	15 000	2.65	5.85	8.54	12.39	306	90	23.8	78.2	.0117	49.4	231	416
130	.60	↓	↓	2.46	5.43	8.58	12.44	307	93	22.2	72.7	.0135	63.2	340	612
131	.50	↓	↓	1.93	4.26	7.76	11.26	303	86	19.0	62.2	.0143	63.1	358	644
132	.40	↓	↓	1.58	3.49	7.34	10.64	296	73	16.0	52.6	.0158	63.0	391	704
133	.65	3048	10 000	3.18	7.00	10.78	15.64	308	94	22.8	74.7	.0115	62.1	287	516
134	.60	↓	↓	2.86	6.31	9.93	14.40	308	95	22.3	73.3	.0121	64.3	312	561
135	.50	↓	↓	2.33	5.14	9.47	13.73	298	77	18.5	60.6	.0120	62.8	303	546
136	.40	↓	↓	1.81	3.99	8.90	12.91	304	87	15.5	50.9	.0154	64.1	389	700
137	.30	↓	↓	1.34	2.95	8.72	12.65	302	84	11.6	38.2	.0232	73.6	640	1152

TABLE VIII. - EXPERIMENTAL WINDMILLING IGNITION DATA - SIMPLEX NOZZLE COMBUSTOR

Nominal flight conditions				Combustor inlet conditions								Combustor operation results			
Run	Flight Mach number	Altitude		Airflow rate		Pressure		Temperature		Reference velocity		Fuel-air ratio required	Combustion efficiency, percent	Temperature rise after ignition	
		m	ft	kg/sec	lb/sec	N/cm ²	psia	K	°F	m/sec	ft/sec			K	°F
138	0.90	7620	25 000	3.13	6.90	8.60	12.47	306	90	28.0	92.0	0.0130	77.4	399	719
139	.80	↓	↓	2.62	5.77	7.74	11.72	304	88	26.1	85.7	.0129	71.9	368	663
140	.70	↓	↓	2.05	4.51	6.18	8.97	304	87	25.4	83.3	.0173	77.2	519	935
141	.70	↓	↓	2.01	4.44	6.00	8.70	307	92	26.0	85.2	.0195	76.9	574	1034
142	.90	6096	20 000	3.70	8.16	10.17	14.75	306	90	27.7	91.0	.0112	72.3	327	589
143	.80	↓	↓	2.95	6.51	8.36	12.12	301	82	26.8	87.8	.0135	79.3	424	764
144	.80	↓	↓	3.03	6.67	8.63	12.52	299	79	26.1	85.6	.0123	75.9	388	698
145	.70	↓	↓	2.55	5.63	7.32	10.62	303	85	26.3	86.3	.0137	74.2	402	724
146	.50	↓	↓	1.58	3.49	6.40	9.28	303	86	18.9	61.8	.0173	75.4	507	912
147	.80	4572	15 000	3.66	8.06	10.38	15.05	308	94	27.4	89.9	.0118	80.3	379	682
148	.70	4572	15 000	3.09	6.82	9.05	13.12	308	95	26.6	87.2	.0117	73.6	346	623
149	.50	4572	15 000	1.93	4.25	7.60	11.02	312	101	20.3	66.6	.0123	64.8	319	575